ČESKÉ VYSOKÉ UČENÍ TECHNICKÉ V PRAZE

Fakulta elektrotechnická
Katedra měření

ZADÁNÍ DIPLOMOVÉ PRÁCE

Student:	**Bc. Jan Novotný**
Studijní program:	**Kybernetika a robotika**
Obor:	**Senzory a přístrojová technika**
Název tématu česky:	**Simulátor kabelů pro železniční prostředí**
Název tématu anglicky:	**Cable Simulator for Railway Environment**

Pokyny pro vypracování:

Navrhněte a realizujte simulátor chování kabelu v železničním prostředí. Proveďte rozbor chování kabelu z hlediska indukování rušivých napětí z vnějších zdrojů signálů nacházejících se poblíž železniční trati. Navrhněte zapojení simulující chování kabelových vedení položených podél kolejí. Na základě toho navrhněte kompletní obvody simulátoru včetně potřebného transformátoru. Simulujte činnost zařízení v programu SPICE. Srovnejte výsledky simulace s chováním realizovaného zařízení - simulátoru kabelu.

Seznam odborné literatury:

[1] Mellit, B., et al.: Computer-based methods for induced-voltage calculations in AC railways. In: IEE Proceedings B-Electric Power Applications. IET, 1990. p. 59-72.

[2] Rashin, Muhammad H.: Power electronics handbook. Elsevier Science, 2011.

Vedoucí diplomové práce:	doc. Ing. Jan Fischer, CSc.
Datum zadání diplomové práce:	18. ledna 2017
Platnost zadání do[1]:	30. září 2018

L. S.

Prof. Ing. Jan Holub, Ph.D.
vedoucí katedry

Prof. Ing. Pavel Ripka, CSc.
děkan

V Praze dne 18. 1. 2017

---

[1] Platnost zadání je omezena na dobu tří následujících semestrů.

Academic year **2016-17**

MASTER PROJECT ASSIGNMENT

Student: **Bc. Jan Novotný**

Study programme: **Cybernetics and Robotics**
Specialisation: **Sensors and Instrumentation**

Title of Master Project: **Cable Simulator for Railway Environment**

Simulátor kabelů pro železniční prostředí (in Czech)

Guidelines:

Design and implement a simulator of behavior of cables in railway environment. Carry out an analysis of the cable behavior in terms of induced voltage interference from external sources of disturbances located near the railway track. Design a circuit simulating the behavior of cables lying along the track. Based on the results, design the complete cable simulator, including required transformer. Run a simulation of the device in SPICE Compare the results of simulation with the behavior of the created cable simulator.

References:

[1] Mellit, B., et al.: Computer-based methods for induced-voltage calculations in AC railways. In: IEE Proceedings B-Electric Power Applications. IET, 1990. p. 59-72.

[2] Rashin, Muhammad H.: Power electronics handbook. Elsevier Science, 2011.

Master Project Supervisor: doc. Ing. Jan Fischer, CSc.

Date of issue: January 18th 2017

Valid until[1]:   September 30th 2018

L. S.

Prof. Ing. Jan Holub, Ph.D.   Prof. Ing. Pavel Ripka, CSc.
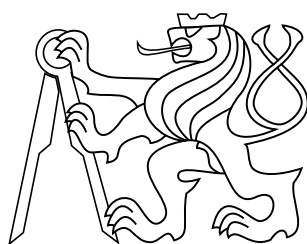   Head of Department   Dean

Prague, January 18th 2017

_____

[1] Assignment validity is limited to three consecutive terms.

master's thesis

Cable Simulator for Railway Environment
Simulátor kabelů pro železniční prostředí

Bc. Jan Novotný

May 2017

Supervisor: doc. Ing. Jan Fischer, CSc.

Czech Technical University in Prague
Faculty of Electrical Engineering, Department of Measurement

Acknowledgement

Declaration

I declare that I worked out the presented thesis independently and I quoted all used sources of information in accord with Methodical instructions about ethical principles for writing academic thesis.

Abstract

Práce se zaměřuje na problematiku simulace chování železničních kabelů. Je zde proveden teoretický rozbor vlastností kabelů používaných v železničním prostředí a vnějších vlivů negativně ovlivňujících připojená zařízení. Na základě teoretického rozboru je proveden návrh laboratorního zařízení, které slouží k testování železničních zařízení v obdobných podmínkách, jakým jsou vystavena při provozu v železničním prostředí. Vlastnosti navrženého simulátoru kabelů jsou změřeny a srovnány se simulovanými předpoklady.

Klíčová slova

Simulátor kabelu, simulace, železnice, indukované napětí, železniční komunikace

Abstract

This work studies the issues of simulating cables in railway environment. A theoretical analysis of the properties of cables used in railway environment and external disturbances influencing connected devices is performed. Based on the result of the theoretical analysis a laboratory equipment used to stress test devices under similar conditions as in the railway environment is designed. The properties of the designed testing device are verified against simulated results.

Keywords

Contents

Nomenclature

Symbols

α	Heat transfer coefficient [W m^{-2} K^{-1}]
μ_0	Permeability of vacuum [H m^{-1}]
μ_r	Relative permeability [-]
ρ	Density [kg m^{-3}]
A_l	Effective cross sectional area [m^2]
B	Magnetic flux [T]
C	Capacitance [F]
C_M	Line to line capacitance [F]
C_G	Line to ground capacitance [F]
c_p	Specific heat at constant pressure [J kg^{-1} K^{-1}]
d	Diameter [m]
f	Frequency [Hz]
I	Current [A]
L	Inductance [H]
l	Length [m]
$LMTD$	Logarithmic mean temperature difference [K]
m	Weight [kg]
N	Count [-]
P	Power [W]
r	Radius [m]
r_k	Induced voltage reduction factor [-]
r_S	Effective area reduction factor [-]
R	Resistance [Ω]
S	Surface area [m^2]
sm	Signal shape multiplier [m^2]
T	Temperature [°C]
T_e	Turns per volt [V $^{-1}$]
U	Voltage [V]
$\dot{V}$	Volumetric flow [m^3 h^{-1}]
V_{RMS}	Effective Voltage

Subscripst

Cu	Copper
diff	differential
Fe	Steel core
M	Maximal
mag	Magnetizatio
n	All membersn
Prim	Primary
sat	Saturation
Sec	Secondary
ser	Series
Tot	Total

Abbreviations

AC	Alternating current
AE	Auxiliary equipment
ESR	Equivalent series resitance
EUT	Equipment under test
RMS	Root mean square

1 Introduction

In the railway environment, there is a need to transmit information and power over long distances. The transmitted information may be for example track status (empty/occupied), point machine position or signal pulses from axle counter. The power transmission considered is powering the motor of point machine or signalization lights. All the systems need to be connected to the control systems via electrical cables.

Goal of this work is to create a laboratory cable simulator to simulate the effect of a cable placed alongside the railway track to test the developed equipment in house and save time and money on testing at specialized testing facilities or to avoid the problems that may be caused by setting the device for field testing without any previous knowledge of its operation with long cables attached. The need for creating custom cable simulator comes from the fact that although there are development centers for railway trackside equipment, no device for this purpose is currently available on the market or no comprehensive phenomena based requirements are available for such a device.

Because the hardware is supposed to work for testing of newly developed equipment for the European market, the frequencies of operation should range from 16.7 Hz for Germany, Austria, Switzerland and Norway to 50 Hz operation for the rest of the Europe using AC electrified tracks. As it is not expected to cause any problems during the development, the cable simulator should support also testing of devices for the 60 Hz systems used for example in Canada, Japan, South Korea, Mexico, Taiwan and United States of America.

To model the behavior of the cable, the properties of the cables will be examined, namely its resistance, capacitance and inductance of the cable. To model the behavior of the cable alongside electrified tracks, the effect of induced voltage from traction current will be explored. The issue of induced voltage is described by railway standards EN 50121-4 [1], VDE 0831 [2] and RIL 819.0804 [3]. The standards however only state that the maximum induced voltage can be 250 V_{RMS} and don't mention the cable topology or length of the cable. Therefore to understand the effects if the induced voltage in greater detail and the variations between different applications, the properties of induced voltage will be analyzed.

The commonly used wire for these applications was defined by development engineers from Siemens s. r. o., is a copper wire with diameter of $1,8$ mm and therefore the goal of this thesis is to create a cable simulator of the 1.8 mm cable for different lengths. These lengths were specified by development engineers from Siemens s. r. o. based on the requirements for their work. The cable lengths should be approximately 100 m, 1 000 m, 3 500 m and over 7 500 m. To keep the size of the cable simulator within size limits each length of cable should consist of only four wires to allow connection of point machine or communication equipment. The current rating of the simulated cables should allow connection of point machine motor so it should handle at least 1 A.

2 Theoretical analysis

In this chapter the properties of the cables and the effect of induced voltage are analyzed. The most important properties of the cable are its resistance, capacitance and inductance so these properties are explored. To explore the effect of induced voltage a finite element method simulations are conducted.

2.1 Parameters of commonly used cables

To find the parameters of the commonly used cables, first the definition of the cable that shall be simulated was needed. This definition of the commonly used cable was provided by development engineers from Siemens s. r. o. as a cable with copper wires with diameter 1.8 mm. The number of wires in the bundle varies greatly according to each installation but to keep the complexity of the cable simulator low while allowing connection of the equipment than needs to be tested, the simulated cable should contain four wires. Further it was specified that the wires are separated within the cable bundle into segments of four wires called quads. This information has been confirmed in the railway cable catalogs [4] an [5] where the cables are listed both with quad distinction and without it. Therefore the requirement of having four wire cable comes also from the mechanical construction of the railway cables.

2.1.1 Resistance of the cable

Main parameter that characterizes all cables is an electrical resistance. Commonly all cables used for telecommunication and signaling equipment are made from copper and the resistance of the wire is defined by its cross-sectional area and its length. Overview of commonly used cables in railway environment is given in [6] where it is analyzed that the used cables have cross-section area from 0.6 mm^2 with resistance from 28.9 $\Omega\ km^{-1}$ to 16 mm^2 with resistance 1.16 $\Omega\ km^{-1}$. Results of this overview correspond with catalogues of railway cable manufactures [4] and [5]. List of commonly used wire sizes and corresponding resistances is in Tab. 1.

Table 1 Resistances of commonly used wire sizes

Wire diameter [mm]	cross-section [mm^2]	Resistance [$\Omega\ km^{-1}$]
0.9	0.6	28.9
1.4	1.5	11.9
1.8	2.5	7.2
3.6	10	1.84
4.5	16	1.16

2.1.2 Capacitance of the cable

Because the cables are laid in bundles close together, the mutual capacitance of the wires is the most important property of the wire except for the resistance. The mutual capacitance of the wires depends on the construction of the cables - the properties of the cable shielding and distribution of the wires in the cable bundle. The capacitances are shown in the Fig. 1 where C_M is the mutual capacitance of the wires and C_G is capacitance of the wires to shielding and ground.
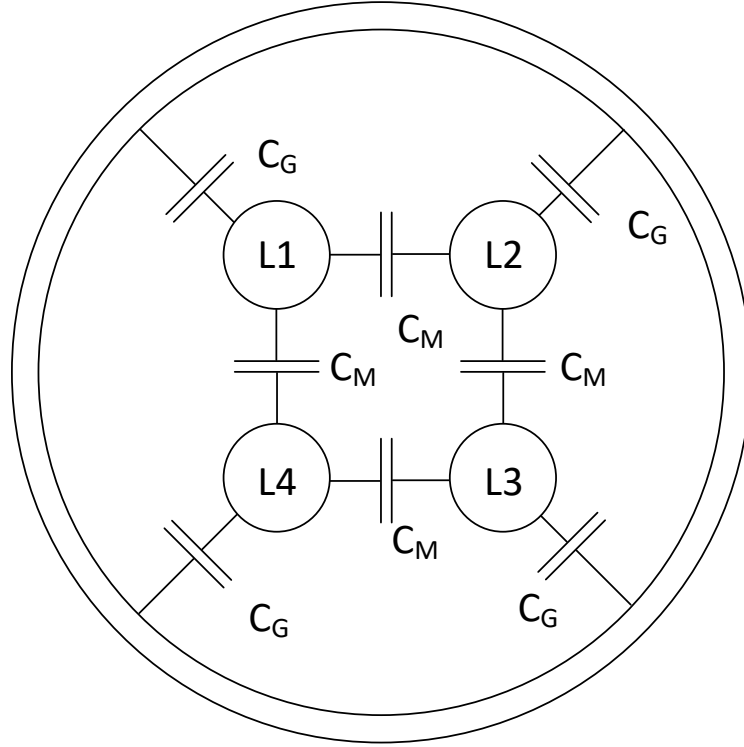

Figure 1 Capacitances between the wires in the cable

This factor is specified by cable manufacturers and is available in product catalogs of railway cable manufacturers [4] and [5]. The total capacitance of wires within railway cables ranges from 45 $nF\ km^{-1}$ to 145 $nF\ km^{-1}$.

2.1.3 Inductance of the cable

Inductance of parallel wires (send and return) has been explored in [7] and [8]. Both sources conclude, that the inductance of two parallel wires can be calculated according to Eq. (1), where d is distance between conductors, r is radius of conductors, μ_r is relative permeability and l is length of the conductors as shown on Fig. 2.

$$L = \frac{\mu_0\ l}{\pi}\ ln\left(\frac{d}{r} + \frac{\mu_r}{4} - \frac{d}{l}\right) \tag{1}$$
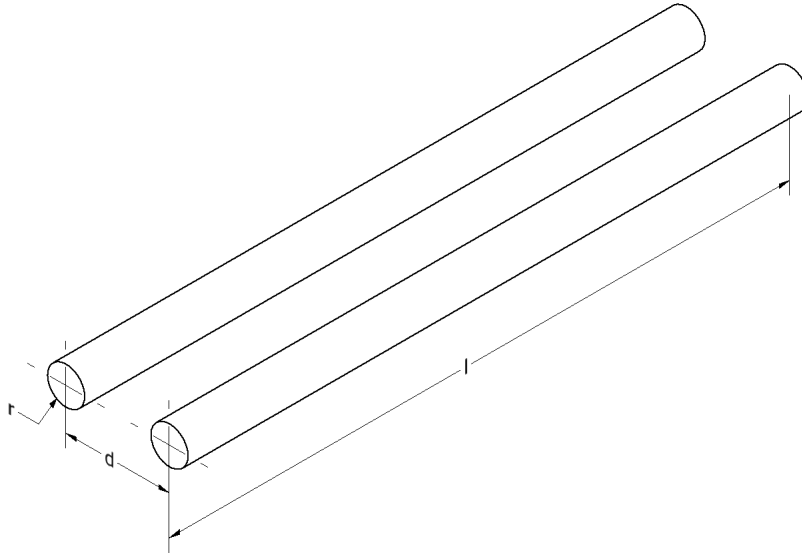
Figure 2 Parallel running set of wires

The value of the wire inductance strongly depends on the diameter of the conductors and the distance between conductors. Because the model of the cable created in this thesis is based on 1.8 mm cable, the only variable is the distance between the wires. From description in the cable datasheets [4] and [5], the distance between the wires ranges from 2.5 mm to 10 mm and therefore the value of inductance ranges from 0.5 $mHkm^{-1}$ to 1 $mH\ km^{-1}$ depending on specific cable construction.

2.1.4 Reduction of induced voltage by cable construction

Because the cables are intended for use in environment where high levels of induced voltage are expected, the reduction factor r_k, specifying how much is the induced voltage limited by the cable construction, is already specified in the datasheets of the cables [4] and [5]. The reduction factor is defined by Eq. (2) described in [9]. This reduction factor generally ranges from 0.1 to 0.7 and the cable providing appropriate shielding is selected during project planning of the cable installation not to exceed the limits on the induced voltage specified in norms EN 50121-4 [1], VDE 0831 [2] and RIL 819.0804 [3] as 250 V_{RMS}.

This reduction is usually achieved by wrapping the cable in a steel foil to provide electromagnetic shielding and in a copper foil to provide electrostatic shielding.

One might think that twisting the wires in the cable might also have some effect on the induced voltage but that is not the case because it's common mode voltage that is almost the same on both wires regardless of the construction.

$$r_k = \frac{Voltage\ induced\ after\ the\ cable\ has\ been\ shielded}{Voltage\ induced\ in\ unshielded\ cable} \tag{2}$$

2.2 Effect of induced disturbing voltages

The induced disturbing voltages can be caused by two main factors: by the induced voltage caused by traction current flowing at the frequency of the supply voltage, by shorting the overhead catenary and causing large current flow trough the catenary and the tracks and by the induced voltage caused by non-harmonic current consumption of the trains.

The effect of the induced voltage caused by the short circuiting of the catenary is not considered in the scope of this work because the transient behavior of power supply circuitry is subject to regulations so the stress limits on on the cables are defined by the regulatory norms.

The effect of induced voltage caused by train drive control and non-harmonic current consumption has not been examined in this thesis because it may vary with each locomotive and the development of drive control is subject to its own normative regulation and standardization. Therefore the effect on the induced voltage in parallel wires should be minimal.

The effect of induced voltage has been simulated in 2D finite element method magnetic simulation software FEMM 4.2 [10], that uses finite element method to solve Maxwell equations describing electromagnetic problems. Meshing is done by triangle software package [11], that creates triangular mesh with automatic size control based on coarseness settings. Models of a railway track with 1435 mm gauge, R 65 [12] rails and an overhead catenary at height 5.5 m have been created. Most of the simulations were done for 1 *km* track segment to obtain per kilometer results of induced voltage as the magnitude of induced voltage is expected to be linearly proportional to track segment length.

Single track, dual track and quad track models were created. These models are based on typical track configuration described in [13]. The topology of single track railway is shown in Fig. 3. The topology of dual track railway is shown in Fig. 4. The topology of quad track railway is based on the same distances between tracks and the height of the overhead catenary as shown in Fig. 4 but not shown here as it would be superfluous. The amplitude of induced voltage is recorded only for positions below the bottom of the tracks because the cables are usually placed in utility channels placed at the edge of the bank.

One case of a singe electrified track and signal cable placed 2 *cm* below the ground surface is shown in Fig. 5. The traction current is 3 kA according to ČSN EN 50388 [14] with the return current evenly distributed between both of the rails.

To obtain the resulting induced voltage a script was made to run the simulations, move the cable within specified area and record the position of the wire and the induced voltage on the cable. The results were acquired even for places where no cable can possibly be installed because the position would interfere with sleepers or other installation equipment. This was done to simplify the execution script and the exclusion of these areas would require changes in the script and could hide some possibly interesting information.

The electromagnetic shielding of the cables wasn't modeled in this phase because the effect of the shielding can be easily expressed by Eq. (3) that is a rearranged Eq. (2).

$$Induced\ Voltage\ shielded = Induced\ Voltage\ unshielded \cdot r_k \qquad (3)$$

The generated mesh was composed of triangles with variable mesh density. The density of the mesh was automatically controlled by the simulation software and is
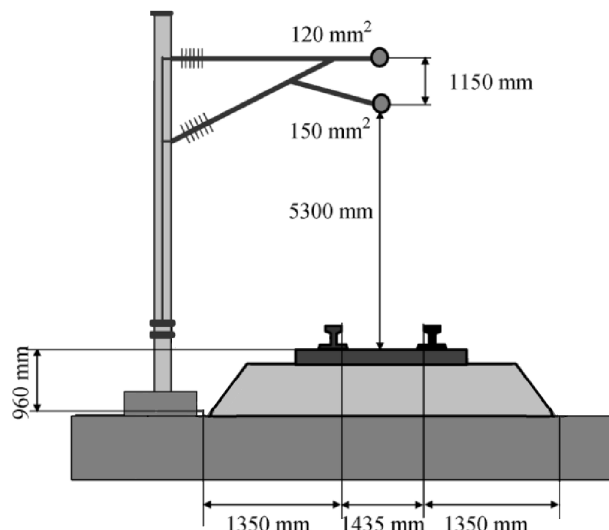
Figure 3 Typical cross section of single track railway (modified from [13])
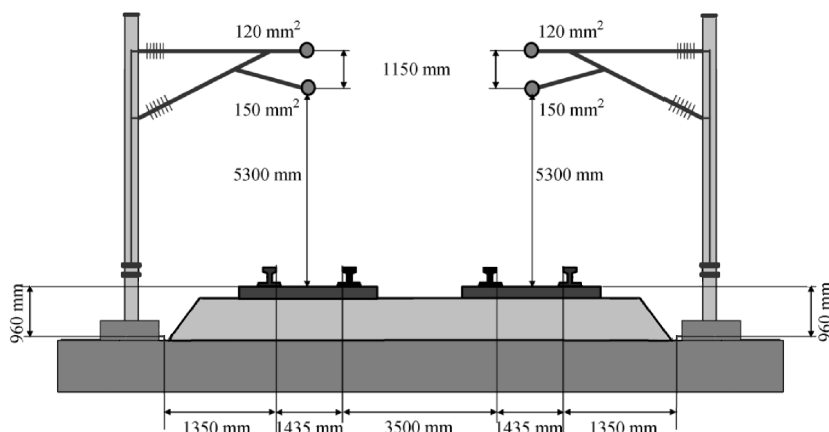

Figure 4 Typical cross section of double track railway (modified from [13])

increased near every vertex on the material edge in the simulation domain. A detail of the generated mesh near one rail is shown in Fig. 6.

Outer boundary conditions of the model were automatically generated by the FEMM [10] software as a seven layer open boundary to simulate infinite free area around the domain of the model.

2.2.1 Material properties in the model

Material properties for air, copper for the overhead catenary and steel for the rails have been taken from FEMM [10] materials library. The gravel/soil properties weren't available in FEMM materials library and therefore are based on information found in [15] and [16]. The parameters for either soil or gravel are very similar with relative permeability $\mu_r = 1$ and conductivity in the range of $\sigma = 1$ to $10\ mS\ m^{-1}$.

The effect of electrical conductivity on the induced voltage has been examined for $1\ km$ long $0.6\ mm^2$ copper cable placed in the middle of the rails and $2\ cm$ below ground at frequency $50\ Hz$. Results from the simulations with conductivity ranging
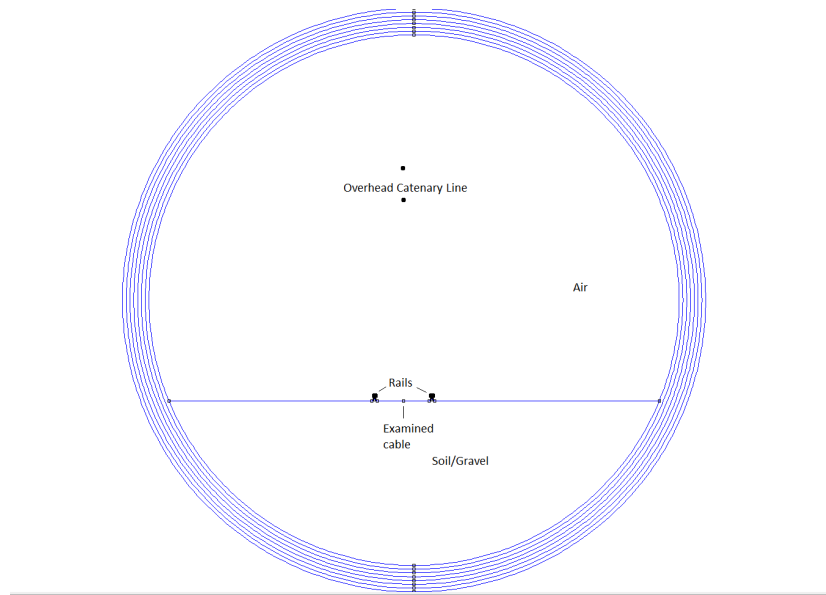
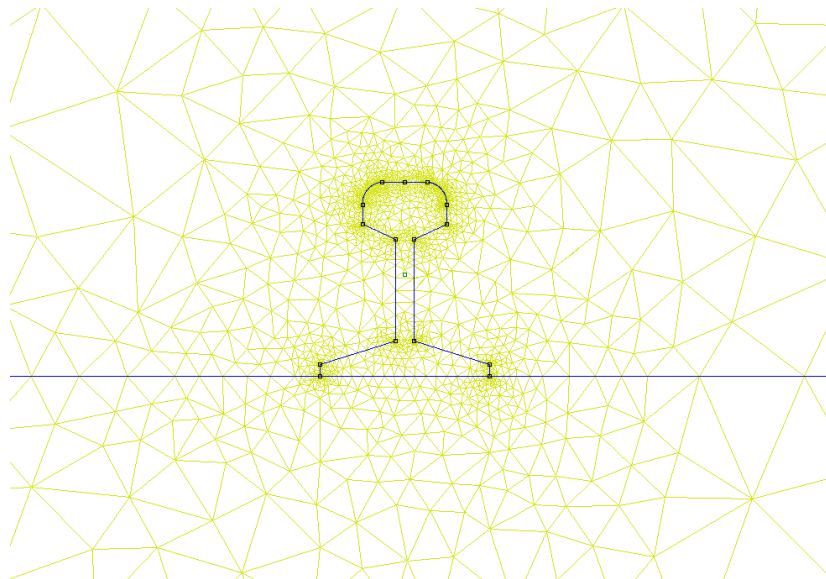**Figure 5** Domain of the simulated single track railway

Figure 6 Detail of the generated mesh near the rail

from 0.1 $mS\ m^{-1}$ to 100 $mS\ m^{-1}$ are in Tab. 2. It is obvious that the conductivity has no effect on induced voltage so the value of 1 $mS\ m^{-1}$ has been chosen.

Table 2 Effect of earth conductivity on induced voltage

Earth conductivity $[mS/m]$	100	10	1	0.1
Induced voltage $[V]$	260.4	260.4	260.4	260.4

2.2.2 Modeling the induced voltage

2.2.2.1 Verification of independence of the solution on mesh size

To verify effect of mesh density on induced voltage a number of simulations with different mesh sizes has been performed. The effect of mesh density on the value of induced voltage has been examined for 1 km long 0.6 mm^2 copper cable placed in the middle of the rails in depth 1 cm at frequency 50 Hz. Results of the simulation are in Tab. 3 and shown in diagram in Fig. 7.

Table 3 Effect of mesh density on induced voltage

Num. of nodes in mesh	17 279	24 381	62 695	215 462	818 110
Induced voltage [V]	440.74	441.45	441.50	441.52	441.54

The difference between the smallest mesh and the largest mesh is less than 0.2 %. Based on this fact and the difference in processing time of several orders of magnitude, the second lowest mesh density has been chosen for all FEMM simulations in this thesis.
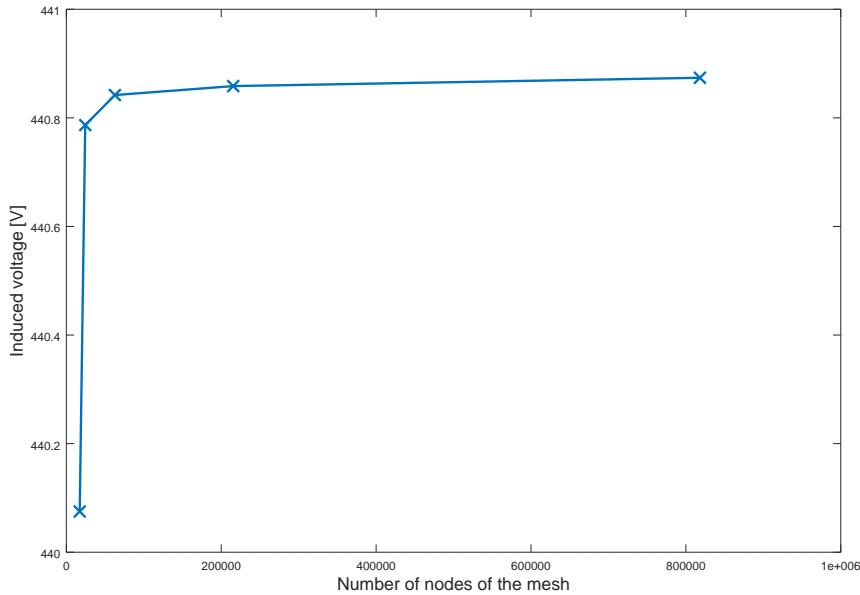

Figure 7 Sensitivity of induced voltage on mesh density

2.2.2.2 Effect of wire length on induced voltage

To verify the assumption that the induced voltage scales linearly with length of the cable, a set of simulations with cable placed in the axis of the track, 20 cm below the ground level. Induced voltage has been noted in Tab. 4. The results show the induced voltage scales linearly with the length of the track segments of length from 100 m to 10 000 m as shown on Fig. 8.

Table 4 Influence of length of the wire on magnitude of induced voltage

Wire length $[m]$	100	500	1 000	3 250	6500	10 000
Induced voltage $[V]$	25.9	129.5	259.1	841.8	1 684	2 590
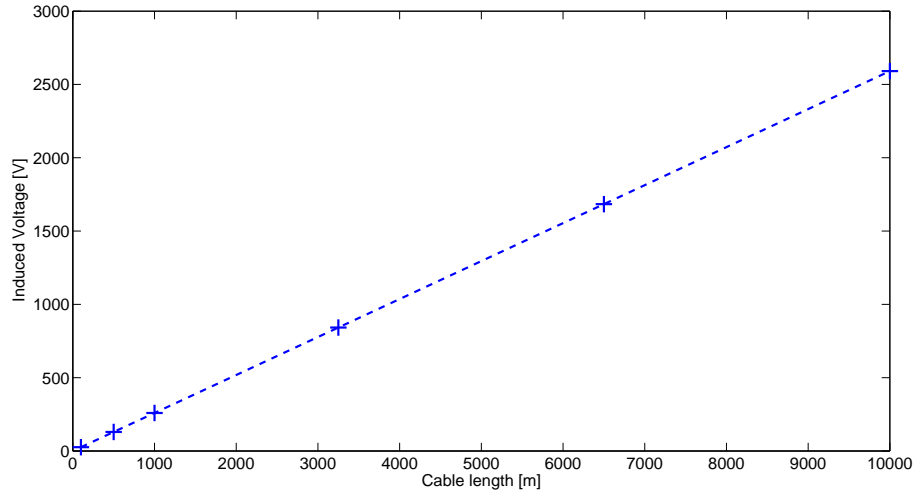
Figure 8 Effect of cable length on induced voltage

2.2.2.3 Effect of wire diameter on induced voltage

The effect of wire diameter on the value of induced voltage has been examined for 1 km long copper cable placed in the middle of the rails in depth 2 cm at frequency 50 Hz. Results of the simulation are in Tab. 5. The difference between the smallest cable 0.6 mm^2 and the largest cable 40 mm^2 is 0.08 %.

Table 5 Influence of cross section of the wire on magnitude of induced voltage

Wire c.s. $[mm^2]$	0.6	1	1.5	2.5	4	6	10	15	20	40
Ind. volt. $[V]$	260.1	260.0	260.0	260.0	260.1	260.1	260.1	260.2	260.2	260.2

2.2.2.4 Effect of number of wires in the bundle on induced voltage

To evaluate the influence of number of wires in a bundle on the induced voltage, a simulation was run with 1 km long, 0.6 mm^2 wires arranged in a bundle of 1 to 16. Examples of wire bundled in the cable are shown in Fig. 9. Results of the simulations are stated in Tab. 6. Twisting of the wires in the bundle that could lower the induced voltage by addition and subtraction of the same voltage along the wire length is not explored here as its effect would be already included in the induced voltage reduction factor provided by cable manufacturer. This reduction factor has been described in chapter 2.1.4.

Table 6 Influence of cross section of the wire on magnitude of induced voltage

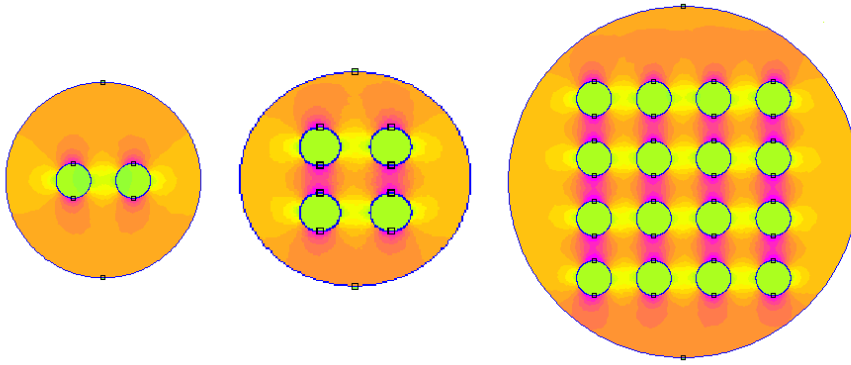| Wire count in bundle	1	2	4	6	9	16
Induced voltage $[V]$	259.1	259.0	259.1	259.0	258.9	258.9

Figure 9 Examples of examined wire bundles with indicative representation of magnetic flux density

The results show that number of wires in the bundle has negligible effect of 0.08 % in the examined range from 1 to 16 wires in the cable bundle. This effect is further examined and discussed by Mellit, et al. in [17] where is shown that depending on the situation, the effect of bundling more cables together can have no, negative or positive effect on the induced voltage but the differences are low enough to be considered negligible.

2.2.2.5 Effect of the frequency on induced voltage

To characterize the effect of frequency of traction current on induced voltage, number of simulations were run at different frequencies from 16.7 Hz to 60 Hz with 1 km long 0.6 mm^2 cable. To check if the difference in frequency has different effect on the induced voltage anywhere around the cable the simulations were done with a script that moved the cable and run the simulation to provide a map of induced voltage for an area around the electrified railway track. Results of the simulations are shown in Figures 10 to 12.
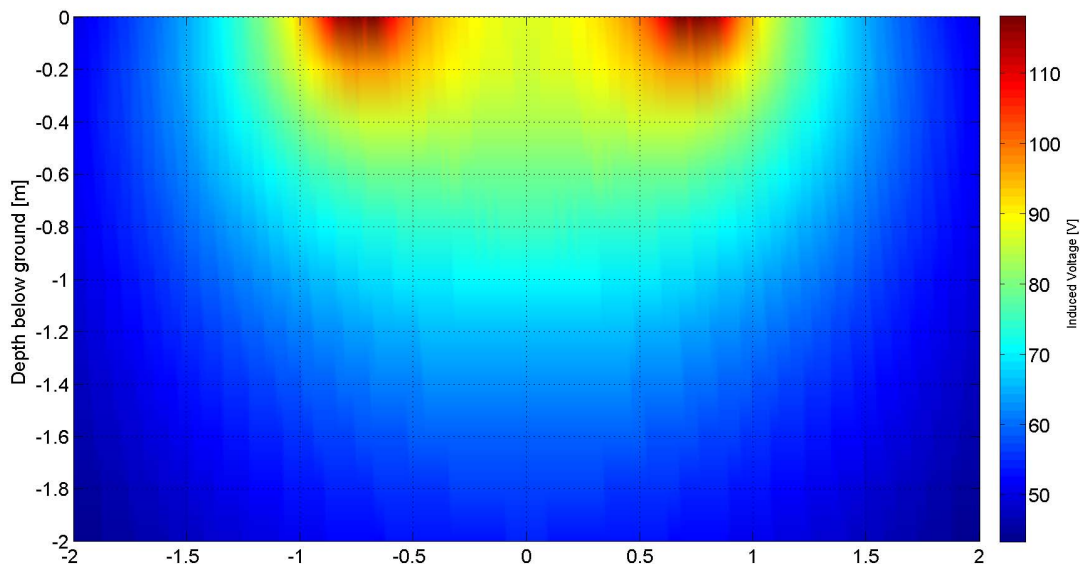

Figure 10 Distribution of induced voltage at f=16.7 Hz and length 1 km
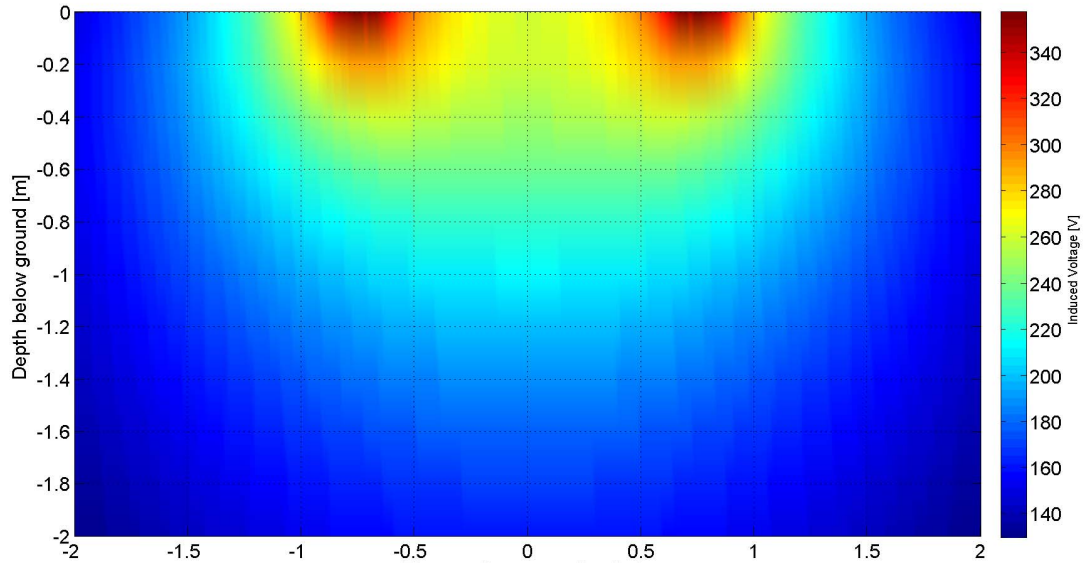
Figure 11 Distribution of induced voltage at f=50 Hz and length 1 *km*
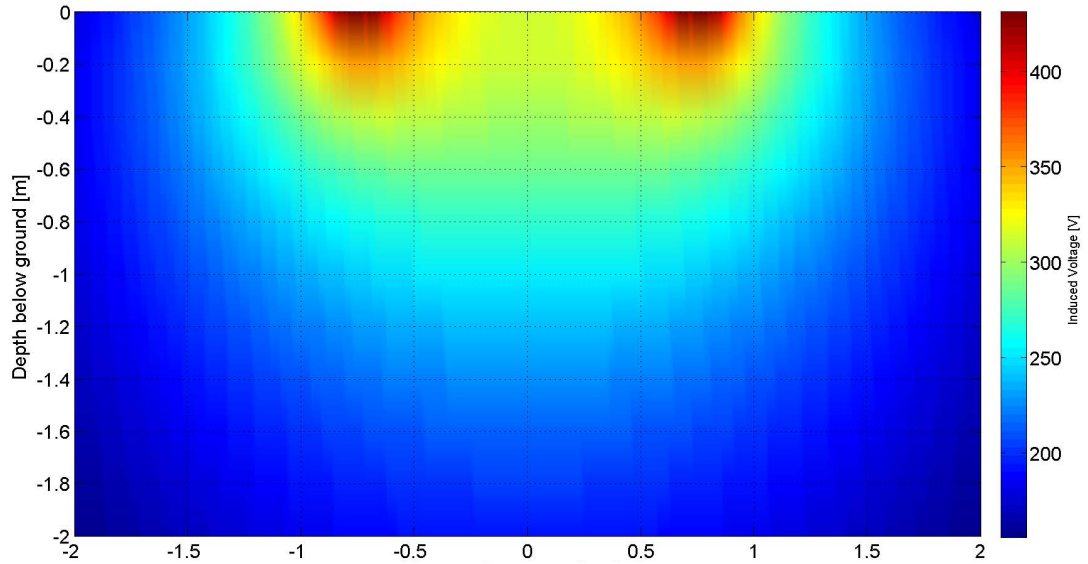

Figure 12 Distribution of induced voltage at f=60 Hz and length 1 *km*

To verify the linearity of the change in induced voltage with change in frequency, the results from 60 *Hz* simulation were taken and multiplied by 16.7/60 to obtain expected reaction at 16.7 *Hz*. The difference between the expected value and the value received is plotted in Fig. 13.

The difference between expected value and obtained value is less than 1 % except for the area directly adjacent to the rails, where the difference is below 3 %. This shows that the distribution of induced voltage is independent of operating frequency of the railway track and therefore results for all frequencies can be obtained from simulation at single frequency with very good accuracy.

2.2.2.6 Effect of Track topology on induced Voltage

The simulations for single track have already been done in chapter 2.2.2.5 so only double track and quad track simulations are done here. Because it was already shown that
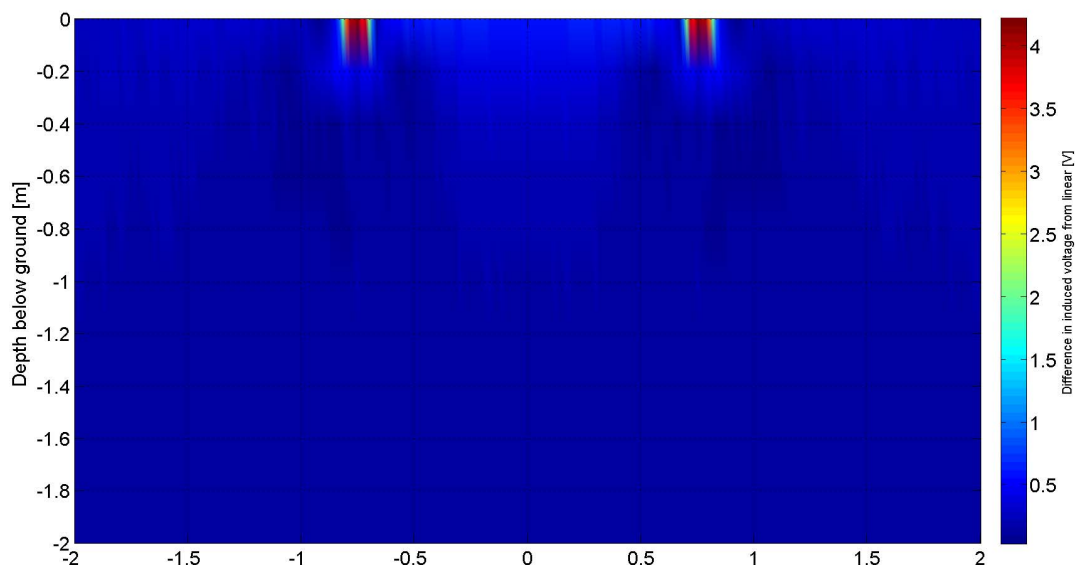
Figure 13 Difference between expected induced voltage at 16.7 Hz obtained from simulation at 60 Hz and induced voltage obtained from simulation at 16.7 Hz.

the results scale linearly with track section length and frequency of the system, only simulation at frequency 50 Hz and length 1 km are done. Plot of induced voltage for dual track railway is shown in Fig. 14 and quad track railway is shown in Fig. 15.
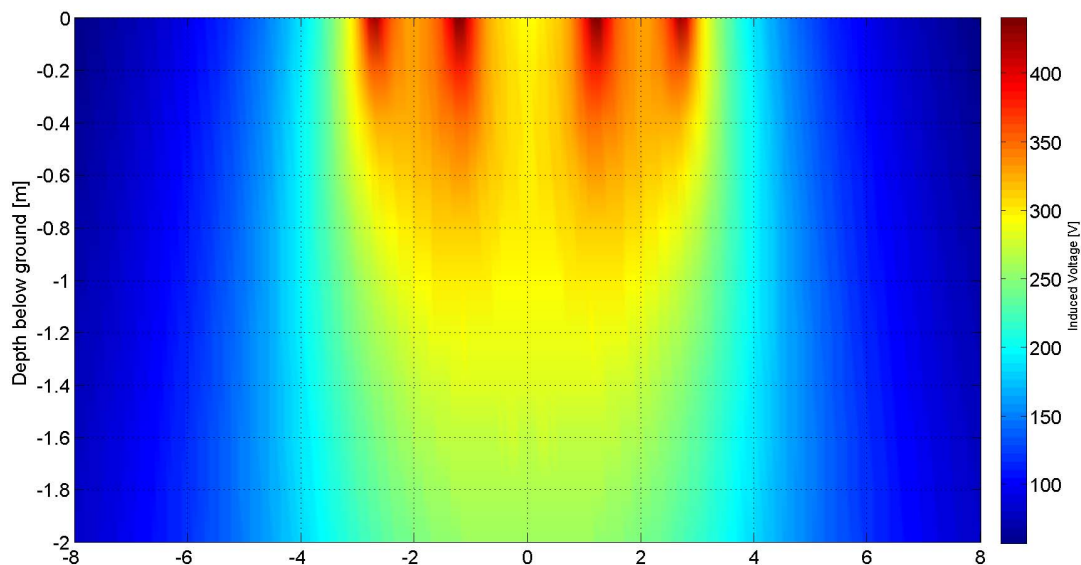

Figure 14 Distribution of induced voltage under double rail track at $f = 50\ Hz$ and length 1 km

Main difference in the behavior of induced voltage between the single track and multi rail tracks is that the magnitude of induced voltage in not decreasing with depth as much as for a single track railway even though it decreases with the same slope with horizontal distance from the tracks.

Finally a simulation of distribution of induced voltages above the railway was done. Note that the simulation occupies also the area where the train would be and where nothing can be installed to provide a overview of the situation above the ground and to get a comparison between the behavior of induced voltage below the ground and above
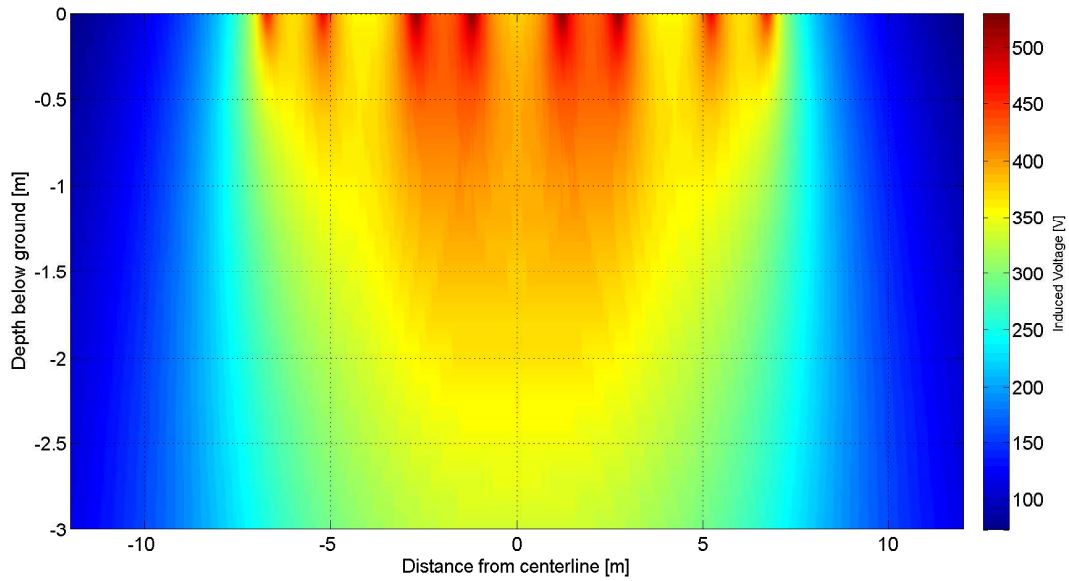
Figure 15 Distribution of induced voltage under quad rail track at $f = 50\ Hz$ and length $1\ km$

the ground. The distribution of induced voltage above ground for $1\ km$ long cable at frequency $50\ Hz$ is drawn in Fig. 16.
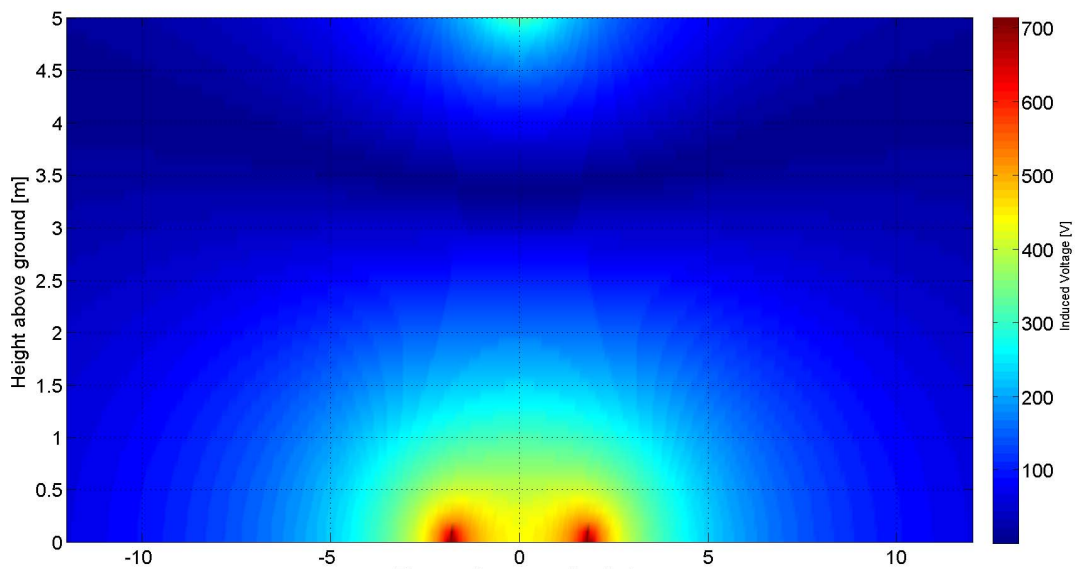
Figure 16 Distribution of induced voltage above single rail track at $f = 50\ Hz$ and length $1\ km$

The results show higher levels of induced voltage, especially in the area directly adjacent to the rails where the voltage levels are double of the induced voltage compared to when the cable is placed under the ground level.

2.2.3 Evaluation of the simulation results

The results from the simulations show that even with unshielded cables the induced voltage can be limited to values required by norms EN 50121-4, VDE 0831 and RIL 819.0804 that state that the induced voltage to cables placed along electrified tracks shall be up

to 250 V_{RMS}, when the cable is placed at least 2.5 m away from the nearest track center line. However not all cable installations can be placed as far from the track, so cables with electromagnetic shielding need to be used. The reduction factor provided by the electromagnetic shielding can be as low as 0.1 [4] and [5], so the magnitude of induced voltage can be reduced up to 10 times. This allows placement of up to 3.5 km cable directly adjacent to the rail or almost unlimited length of cable when restriction to place the cable at least 2.5 m from the track center line is imposed.

Because the upper limit on induced voltage is imposed by the normative regulations as 250 V_{RMS}, the cable simulator should support modeling of induced voltages up to 300 V to test that the devices can safely operate within specified limits with sufficient margin to account for component tolerances and temperature changes during operation.

2.3 Model of the cable

Parameters of cables that need to be considered in the model have been identified in chapter 2.1 as the wire resistance, wire inductance and mutual capacitance of the wires. These parameters have been used to create the model of the cable itself. In this work a simulator for approximately 100 m, 1000 m, 3000 m and 7500 m cables, each containing four signal wires, is created.

In an ideal case the capacitance, resistance and inductance would be distributed continuously to provide the same behavior as the real cable. Because the model needs to fit in limited volume of a laboratory device, the distributed model needs to be simplified into a single segment of lumped element model.

2.3.1 Capacitance of the cable

The mutual capacitance between the cable lines and the line to ground capacitance are distributed according to the cable specifications in [18]. To achieve the ratio of mutual cable capacitance and capacitance of cable to ground, the cable to ground capacitance is considered to be double of the mutual cable capacitance. This is simply achieved by placing two of the capacitors in parallel and so a single value of capacitors can be used for one length of wire.

The simplification of the cable capacitance can be done, by placing a set of capacitors on each end of the cable, while maintaining the total capacitance of the cables as specified in chapter 2.1.2 as 145 $nF \ km^{-1}$. This approach has the advantage of being fairly simple for manufacture while providing sufficient approximation of the cable behavior.

Values of the capacitors in the model C are based on the length of the simulated cable are defined by Eq. (4) to provide the total line capacitance loading of 145 $nF \ km^{-1}$ for the given length of wire. Cable length l is inserted in meters and the result is in Farads.

$$C = \frac{C_{Tot}}{8} = \frac{l \cdot 145 \cdot 10^{-12}}{8} [F] \tag{4}$$

2.3.2 Resistance of the cable

The resistance of the cable presents itself as a purely resistive element placed in series with the cable. This resistance is modeled as a resistor placed in series with each line as shown in the model in Fig. 17.

Value of the resistors R in the cable was described in chapter 2.1.1. It can be expressed according to Eq. (5) to obtain the cable resistance 7.2 $\Omega \ km^{-1}$. Cable length l is inserted in meters and the result is in Ohms.

$$R = R_{Tot} = l \cdot 7.2 \cdot 10^{-3} [\Omega] \tag{5}$$

2.3.3 Inductance of the cable

The inductance of the wires in the cable has been calculated in chapter 2.1.3. To fit the inductance to the lumped element model, the inductance is placed in series with each line as L as shown in the model in Fig. 17. The Fig. 17 show also expected connection of auxiliary testing equipment (AE) and equipment under test (EUT).

Because the wire diameter of examined cable is 1.8 mm, this value can be inserted to Eq. (1), from which the Eq. (6) is obtained. Cable length l is inserted in meters and the result is in Henrys.

$$L = L_{Tot} = l \cdot 752 \cdot 10^{-9}[H] \tag{6}$$
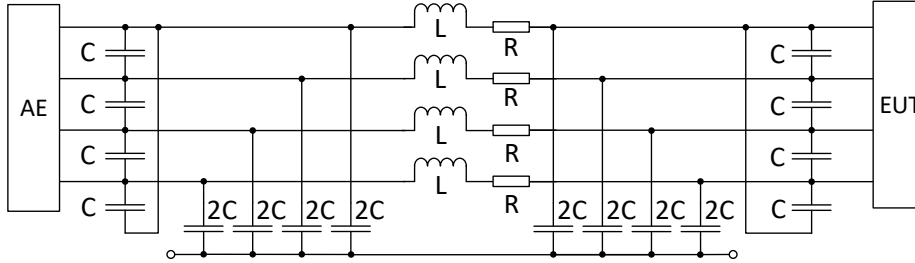

Figure 17 Schematic of the cable model

2.3.4 Complete model of the cable

The values of resistance, inductance and capacitance in the model shown in Fig. 17 for each simulated length of wire are summarized in Tab. 7. Each length of the cable consists of four wires to connect the required devices.

Table 7 Calculated component values for given lengths of cable

Wire lenght [m]	100	1000	3000	7500
Total wire capacitance C_{Tot} $[nF]$	14.5	145.0	435.0	1 087.5
Model capacitance C $[nF]$	1.8	18.1	54.4	135.9
Wire inductance L $[mH]$	0.08	0.75	2.26	5.64
Wire resistance R $[\Omega]$	0.7	7.2	21.6	54.0

To complete the model, the influence of induced voltage has to be added to the model. The issue of induced voltage is explored in chapter 2.2, however the maximum value is defined by norms EN 50121-4 [1], DIN VDE 0831 [2] and RIL 819.0804 [3] as 250 V_{RMS}. To create laboratory device capable of properly testing developed devices, the model shall provide testing induced voltages up to 300 V.

3 Realization of the cable simulator

To create usable laboratory equipment, following requirements were taken into account:

Maximum current per wire	1.5 A
Maximum induced voltage	300 V
Maximum cable voltage	400 V

The cable simulator should be able to simulate a four wire cable of following lengths: 100 m, 1 km, 3 km and 7.5 km.

3.1 Schematic of the cable models

The schematics of each cable length differs in value of components but they all share common schematic, that can be seen in Fig. 18. To provide sufficient safety of operation all capacitors in the simulator are Y2 class. The induced voltage is always distributed across two capacitors, therefore the voltage rating of used capacitors shall be at least $550\ VAC$ as calculated in Eq. (7).

$$400\ VAC + \frac{300\ VAC}{2} = 550\ VAC \tag{7}$$

All available Y2 capacitors are rated at $300\ VAC$. This voltage rating is not sufficient to safely connect required input voltage, therefore two capacitors are connected in series to halve the voltage present on each one. Because the exact capacitance cannot be achieved for the $7900\ m$ cable with available capacitor values, parallel combination of two capacitors is used. Another difference from the model shown in Fig. 17 is that the cable is split in the middle to allow the connection of transformers simulating induced voltage.

When the required capacitances were first calculated to match the required cable lengths, the results were consulted with supervisors. Based on the consultation with supervisors and the capacitance of available Y2 rated capacitors, the lengths of the cables to be simulated by the cable simulator have been altered from the initial requirements to $130\ m$, $1300m$, $2\ 760\ m$ and $7\ 900\ m$. Values of each component used to build the simulator are shown in Tab. 8. The values have been chosen to represent values for each required cable length as closely as possible.

Table 8 Calculated component values for given lengths of cable

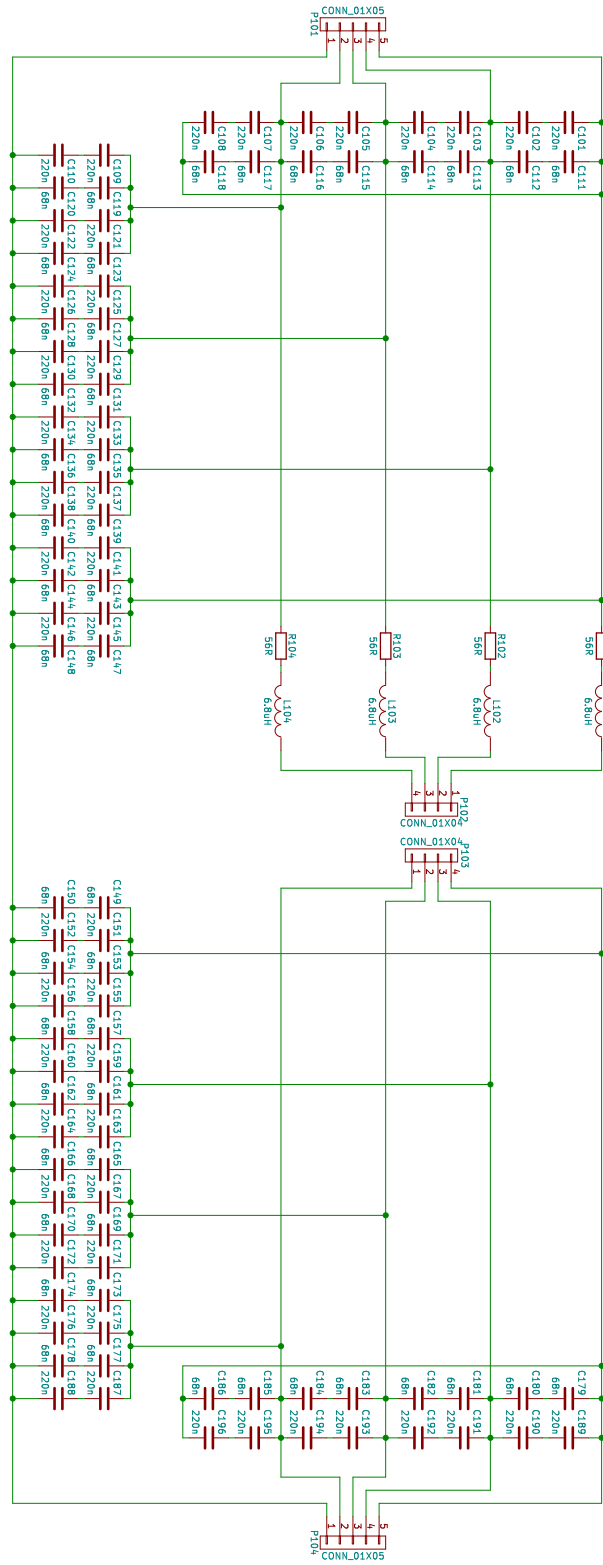| Wire lenght [m]	130	1300	2760	7900
Capacitor value C_n [nF]	4.7	47	100	220+68
Inductors value L_n [mH]	0.1	1	2.2	6.8
Resistors value R_n [Ω]	0.91	10	22	56

Figure 18 Schematic of the 7900 m cable model

3.2 Layout of the cable models

The layout of the cable models has been done in a way that the parasitic effects of the printed circuit boards on the behavior of the cables is minimized. Another factor in the design of the printed circuit boards is the fact that voltages up to 700 V are present in the circuit ad therefore sufficient clearance distances need to be met. Because the cable simulator needs to be safe for operators, reinforced insulation is required.

3.2.1 Insulation

The insulation distances can be divided in two groups: clearance and creepage distance. Creepage distance is the shortest path between two traces along the surface of the base material. This distance can be increased for example by placing slots and cutouts (1 mm minimum to be considered) in the printed circuit board. Clearance stands for the shortest air distance between two traces. Clearance can be increased by placing insulating spacers between the traces.

The creepage distance further depends on pollution degree and material group. The description of pollution degrees is in Tab. 9 based on description from [19]. The materials are classified into classes I, II, $IIIa$ and $IIIb$. The class of the material should be provided by the manufacturer of the printed circuit boards. If the material class is not known, then the worst class $IIIb$ should be assumed.

Table 9 Pollution degrees and its meaning

Pollution degree	description
1	Dry non-conductive or no pollution
2	Non conductive pollution that may temporarily become conductive due to condensation
3	Conductive or wet pollution

The clearance distance is not dependent on properties of the base material and therefore is defined only by the insulation voltage. Usually the clearance distance is larger than the creepage and so it is the one specifying the minimum required trace distance.

3.2.2 Calculation of insulating distances

The operation voltage of the circuit is 700 V AC. The insulation distances can be calculated by using online tools based on relevant normative references. The creepage calculation tool [19] is based on the UL60950-1 [20]. The creepage distance calculated by the tool is 2.4 mm. The clearance is calculated by the tool [21] that is based on the IPC-2221 [22]. The calculated clearance distance is 4.95 mm.

The insulation calculated by the tools above is only the required insulation distance for basic insulation. The cable simulator design requires reinforced insulation to provide safety for the operator, so the trace spacing must be double than the spacing required by the basic insulation. The trace spacing distance is therefore set to the clearance distance 9.9 mm.

3.2.3 Layout of the boards

During the layout phase of the design, the boards were separated to several sub boards to save the board space. The capacitor banks were split to two boards. First one of the

boards contains the mutual capacitance between the wires. The second board contains the capacitance to ground. For the 130 m cables, the power dissipation of the series resistance is low enough, that the resistors don't have to be mounted on heat sink, so the 130 m cable has three different boards, to populate the resistors. All the boards of different lengths of the wire don't contain space for the inductors, because the chosen inductors are with air core and so the area that would be taken on the board would be too high and so the coils will be wire connected off the boards. The other lengths of the cable have only two different boards because the resistors are not mounted on the boards, but on the heat sinks.

The layout of the board simulating the mutual capacitance of the 2760 m cable is shown on Fig. 19. The layout of the board simulating capacitance to the ground of the 2760 m cable is on the Fig. 20.
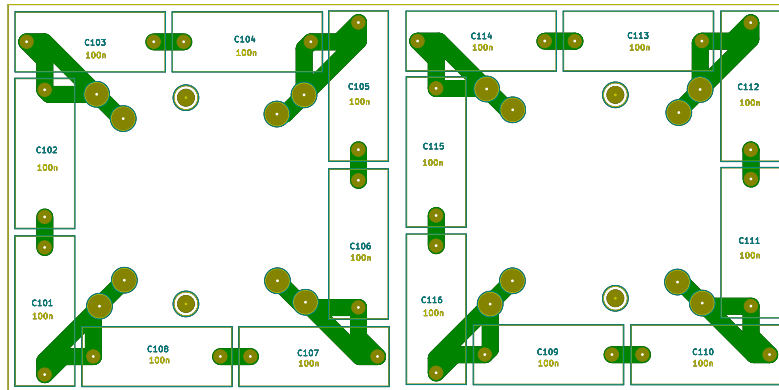

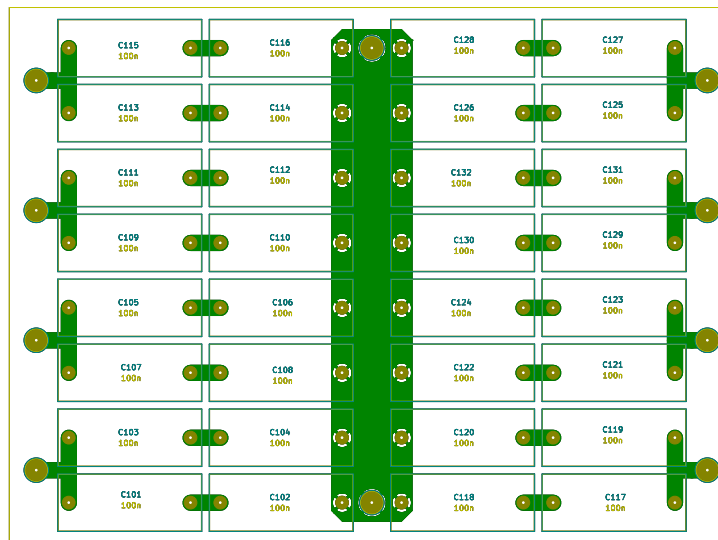**Figure 19** Layout of the 2760 m cable mutual capacitance board

Figure 20 Layout of the 2760 m cable wire to ground capacitance board

3.3 Thermal design of the cable simulator

Thermal design of the wire simulator is done with the assumption that only one length of wire will be used at a time. Therefore the power dissipated by resistive elements in all four lines of the cable is calculated in Eq. (8), where N is number of lines in the cable placed on single heat sink, R_M is maximal series resistance of the line and I_M is maximum continuous current through the line.

$$P_M = N \ R_M \ I_M^2 = 239 \ W \tag{8}$$

To manage the heat generated by the cable simulator a rack-mount box with heat sink side panels has been chosen. The box 1PD03300N from modushop[1] offers one $300x40x120 \ mm$ finned heat sink on each side. To dissipate sufficient amount of heat a fan needs to be added on each heat sink to provide sufficient airflow.

The surface area of all heat sink fins is $S = 0.216 \ m^2$, to compensate for uneven temperature distribution within the heat sink a reduction factor of $r_S = 2/3$ has been added. Convective heat transfer coefficient for heat transfer has been taken from Tab. [23] and Tab. [24], where the value of heat transfer coefficient for forced convection for low speed air flow is $10 \ W \ m^{-2} \ K^{-1}$ and for moderate speed air flow is $100 \ W \ m^{-2} \ K^{-1}$. Because the fan will be facing the heat sink directly, the heat transfer coefficient between slow speed air flow and moderate speed air flow may be used, however because the source doesn't state what air flow speed can be considered slow or moderate, the heat transfer coefficient has been estimated as $\alpha = 50 \ W \ m^{-2} \ K^{-1}$. Given the comparably high thermal resistance of other possible cooling paths for the resistors, the other paths to dissipate the heat generated by the resistors in the cable simulator are neglected for the cooling calculations. Also given that the air-side heat transfer coefficient is the highest resistance in path between the resistors and the air, all other thermal resistances (materials contact, conduction) are considered negligibly small and are neglected.

To calculate logarithmic mean temperature difference a temperature of the heat sink $T_h = 75°C$ and ambient temperature $T_a = 30°C$ are considered. The temperature rise of the air flowing over heat sink ΔT_{air} has been calculated according to rearranged energy balance expressed by Eq. (9), where the heat flow has been halved because the heat sources are evenly distributed to both heat sinks of the box, properties of the air have been taken from the Tab. in [25], so the specific heat of the air at constant pressure is $C_p Air = 1.005 \ kJ \ kg^{-1} \ K^{-1}$, air density is $\rho = 1.2 \ kg \ m^{-3}$. $\dot{V} = 330 \ m^3 \ h^{-1}$ is volumetric flow of the air provided by two 120 x 120 x 38 mm fans[2] mounted on each heat sink. Heat flow to one heat sink has been calculated as half of the total power generated by resistive elements in the cable simulator.

$$\Delta T_{air} = \frac{P_M}{c_{pAir} \dfrac{\dot{V}}{\rho}} = 2.3°C \tag{9}$$

Based on the information the logarithmic mean temperature difference is calculated in Eq. (10).

$$LMTD = \frac{(T_h - T_a) - [T_h - (T_a + \Delta T_{air})]}{ln\left(\dfrac{T_h - T_a}{T_h - (T_a + \Delta T_{air})}\right)} = 43.85°C \tag{10}$$

---

[1]1PD03300N - 3U Krabice s chladičem, 300mm, 4mm-rack černý - http://www.modushop.cz/1PD03300N-3u-krabice-s-chladicem-300mm-4mm-rack-cerny.html

[2]SUNON DP200A2123XBT.GN - http://www.tme.eu/cz/details/dp200a2123xbt/ventilatory-ac-230v/sunon/dp200a2123xbtgn/

Maximal power that can be dissipated by each of the two heat sinks $P_{CoolMax}$ has been calculated according to Eq. (11).

$$P_{coolM} = S \cdot r \cdot \alpha \cdot LMTD = 315.7 \ W \tag{11}$$

From the Eq. (9) to Eq. (11) has been shown that both heat sinks in the rack mount box can dissipate 127 W more or 25 % more than required within specified operation conditions and are therefore sufficient to dissipate the heat from the resistors in the cable simulator when each heat sink is equipped with two 120 mm fans with sufficient margin to cover uncertainties in selecting the heat transfer coefficient for forced convection and reduction factor of surface area to factor out the uneven distribution of temperature in the heat sink.

3.4 Influence of the induced voltage

To simulate the influence of the induced voltage in the laboratory equipment, a transformer with one primary and four secondary windings needs to be used. Because no off the shelf transformer can provide required properties a custom transformer needs to be designed.

3.4.1 Transformer design

The input parameters for the design of the transformer are summarized in Tab. 10. These parameters were chosen in accordance with available laboratory power supplies. The power supply that will be used in the cable simulator is Chroma 61602, that can supply up to 1 000 VA at voltages up to 300 V. The transformer shall be able to provide full 1 000 VA at 250 V and continue operation up to 300 V.

Table 10 Input parameters for design of the transformer

Operating voltage [V]	300
Maximum secondary current per winding [A]	1
Number of secondary windings [$-$]	4
Operating frequency [Hz]	16.7-60
Maximum temperature rise[$°C$]	25
Transformation ratio [$-$]	1:1
Insulation between windings [$kVAC$]	5
Maximal weight [kg]	30

3.4.2 Choosing the core size

Because the transformer should insert as little leakage inductance as possible a transformer wound on toroidal core has been chosen. To get an approximation of the size of the core that is required, an empirical formula for selecting core cross section area A_l shown by Eq. (12) from [26] has been used. Derivation of the formula is shown in [27]. This formula requires to input the operation frequency f, signal shape multiplier sm, maximal magnetic flux density of the core B_M and turns per volt T_e. The signal shape multiplier for sinusoidal waveform is $sm = 4.44$. The initial value of turns per volt to be used in the calculation is recommended in [7] as $T_e = 3\ turns\ V^{-1}$. The maximal magnetic flux density B_M can be obtained from the datasheet of the magnetic cores [28] for a given material. The $SB1$ series material with saturation flux density $B_{sat} = 1.65\ T$ has been chosen. The maximal flux density has been lowered by 15 % to accommodate for variations in the core and to maintain safe operation outside the saturation area, so the maximal magnetic flux density is $B_M = 1.4\ T$.

$$A_l = \frac{1}{sm\ f\ T_e\ B_M} = 30\ 300\ mm^2 \tag{12}$$

Based on the known cross sectional area, the core can be selected from catalog. Description of dimensions of the core are on Fig. 21. Available core sizes are reviewed in the Tab. 11.

The $T2000$ transformer core fits as closest higher match to size calculated by Eq. (12) and so the $T2000$ core has been selected for the transformer.
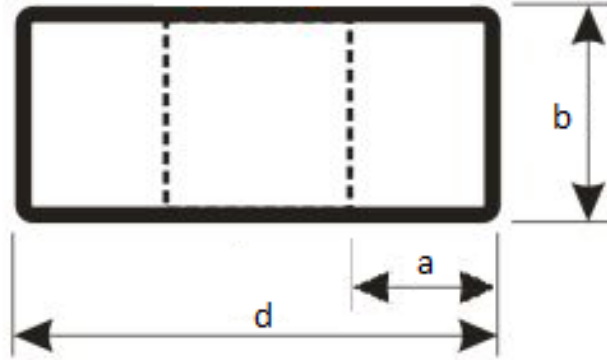
Figure 21 Description of core dimensions

Table 11 Available toroidal cores

Core	a $[mm]$	b $[mm]$	d $[mm]$	A_l $[mm^2]$
T1600	50	60	205	3 000
T2000	50	75	230	3 750
T3000	75	95	240	7 125
T4000	90	130	250	11 700

To get approximate thermal dissipation of the transformer when considering a temperature rise of $\Delta T = 30°C$ has been considered. To get the heat transfer coefficients, the core dimensions were used in calculation tool provided by [23]. The heat transfer coefficients were inserted to the FEMM [10] software to calculate maximal thermal dissipation of the transformer. The simulation resulted in maximal power dissipation of the torus to maintain maximal temperature rise of $\Delta T = 30°C$. The power dissipated at this temperature rise is $P_M = 34.8 \ W$. Results of the thermal simulation is shown in Fig. 22.
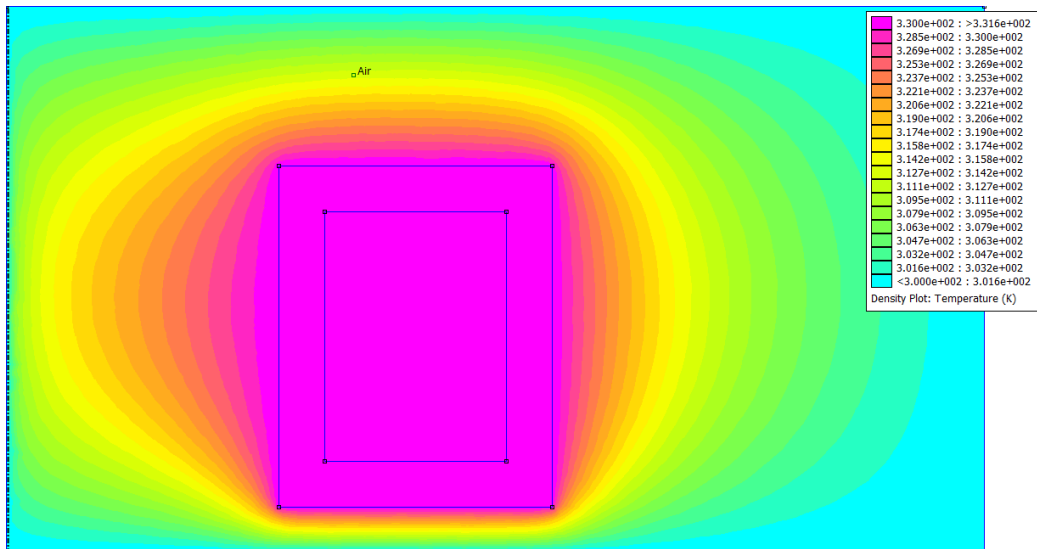

Figure 22 Thermal simulation of the transformer core (Right half cross section)

The volume of the core is $2.12 \cdot 10^3 cm^3$. When considering the density of silicone steel

approximately 7.6 $g\ cm^{-3}$, the weight of the core is $m_{Fe} = 16.2\ kg$. The core losses are specified in the core material datasheet [28] as $W_{10/50} = 0.5\ W\ m^{-1}$. The weight of the core is 16.2 kg and so the core losses are $P_{Fe} = 8.1\ W$. The maximal power dissipation of the copper windings shall therefore not exceed $P_{Cu} = 26, 7\ W$

3.4.3 Calculating windings of the transformer

3.4.3.1 Primary winding

The actual turns per volt can now be calculated from the Eq. (21) by substituting the approximate core area and getting the number of turns per volt $T_e = 2.42\ turns\ V^{-1}$ as a result. In order for the transformer to handle 300 V, the primary shall be at least $N = 727\ turns$. Therefore a primary with $N = 730\ turns$ has been chosen. The magnetization current of the transformer is calculated from Eq. (13) and Eq. (14) from [29] where μ_r is relative permeability, μ_0 is absolute permeability of vacuum, A is cross sectional area of the core and l is mean magnetic length of the core, f is frequency of operation, U is applied voltage and L is the voltage calculated in (13). The magnetization current is $I_{mag} = 0.131\ A$. Because the magnetization current must be added to the dimensioning of the primary coil the current required is 4.131 A.

$$L = \mu_r \mu_0 \frac{N^2\ A}{l} \tag{13}$$

$$I_{mag} = \frac{U}{2\ \pi\ f\ L} \tag{14}$$

In order for the core not to overheat, the maximal resistance of the primary winding R_{CuM} shall not exceed resistance calculated by Eq. (15) as 0.782 Ω.

$$R_{CuM} = \frac{P_{Cu}}{2I^2} \tag{15}$$

The length of wire to provide 730 turns on the core used is 220 m. The diameter of copper wire needed for the length of the wire is 2.4 mm. To improve stacking of the wire around the core, 12 strands of wire with diameter 0.7 mm have been chosen for the primary winding. The amount of copper required cannot be wound on the core of this size so the transformer needs to be designed with larger core.

Calculations for the transformer with larger core are the same as in this example, however it was found that required transformer would weigh at least 40 kg and therefore weight would be over the required 30 kg and so the resulting element of the cable simulator could not be handled by a single person. Solution to the weight problem is to separate the transformer into two smaller transformers, each with single primary and two secondary windings.

The smaller transformers are based on the same $T2000$ core with the same 730 $turns$ on primary side. The maximal resistance of the copper winding to fit the maximum power dissipation of the transformer is calculated by the same Eq. (15) as before, however only $I = 2.131\ A$ is substituted for the current and the maximum possible resistance is 2.94 Ω. The length of the wire is expected to be the same 120 m per winding. The required wire diameter is 1.29 mm, to improve the stacking factor 4 parallel wires of 0.7 mm diameter are used.

To calculate the size of the the primary winding of the transformer, the number of wires that can fit inside the inner radius of the coil is calculated based on its diameter, the diameter of the wire and thickness of insulation of the wire. The thickness of the

insulation is estimated according to [30] as 0.05 mm layer, increasing the diameter of the wire by 0.1 mm to 0.8 mm. To fit 730 turns of 4 parallel strands of 0.7 mm wire, 3 layers of the wire are needed, so the primary winding creates 2.4 mm layer of copper on top of the core.

The total volume of copper wire used for primary winding is $3.4 \cdot 10^2$ cm^3. When considering the density of the copper 8.96 $g\ cm^{-3}$, the weight of the primary winding is $m_{CuPrim} = 3$ kg.

3.4.3.2 Secondary winding

The secondary windings are designed for 1 A. The design is the same as for the primary winding. Each winding is consisting of two parallel strands of wire with diameter 0.7 mm. Each winding consists of two layers of copper wires and therefore each layer adds 1.6 mm on top of the primary winding.

The volume of copper of the first secondary winding is $1.78 \cdot 10^2$ cm^3. The weight of the first secondary winding is 1.6 kg. The volume of copper of the second secondary winding is $1.78 \cdot 10^2$ cm^3. The weight of the second secondary winding is 1.6 kg. The total weight of secondary windings is $m_{CuSec} = 3.24$ kg.

3.4.3.3 Insulation between windings

The required insulation cannot be achieved only by the lacquer layer on the wires. An additional insulation layer needs to be added to the transformer. The Insulation films providing higher breakdown voltage than the required 5 kV are 2.5 mm thick [31]. Because the insulation must be placed between primary and both secondary windings, the total thickness of the insulation layers added to the transformer is 7.5 mm.

3.4.4 Complete design of the transformer

The windings of the transformer shall be wound on the $T2000$ core with 2.5 mm insulation between the windings. All the windings shall be done in the same direction. The electrical diagram of the transformer is in Fig. 23. The description of each winding is in Tab. 12. The stacking of the windings on the core is in Fig. 24 a) and the mechanical diagram showing output placement of the transformer is in Fig. 24 b).
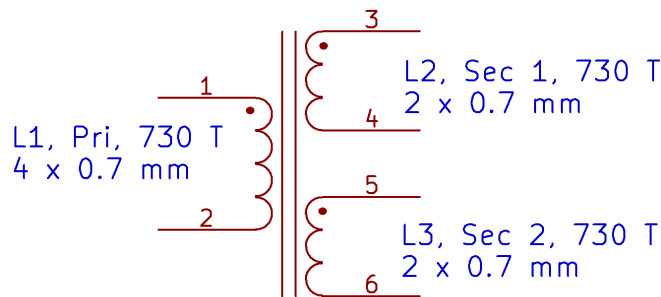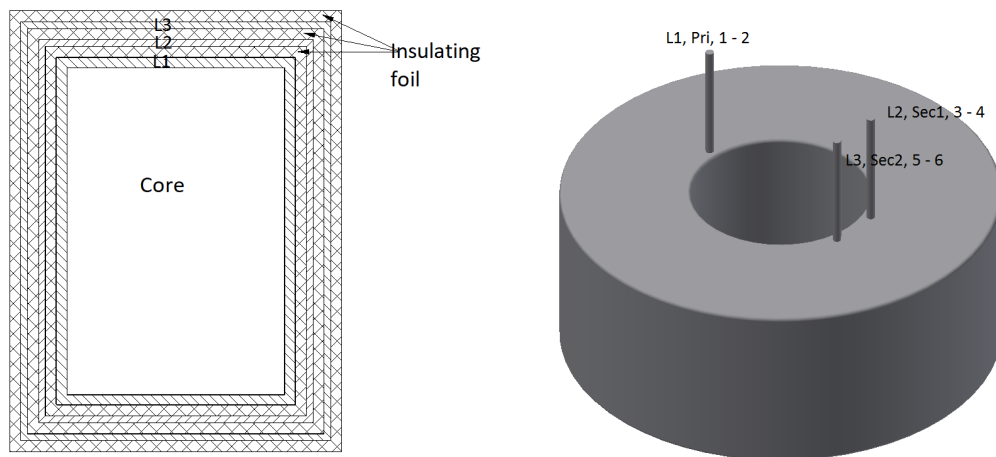

Figure 23 Electrical diagram of the transformer

To verify the weight of each transformer to see if it is lighter than the required 30 kg, the weights of all the copper windings and of the core were summed. The total weight of one transformer is 22.24 kg. This weight fits in the 30 kg limit with sufficient margin for the rack mounted box the transformer will be placed in.

Table 12 Description of transformer windings

Winding	Number of turns	Wire diameter [mm]	Number of strands	Layer count
L1, Pri	730	0.7	4	3
L2, Sec1	730	0.7	2	2
L3, Sec2	730	0.7	2	2

a) Stackup of windings on the core   **b)** Mechanical diagram of the transformer

Figure 24 Mechanical construction of the transformer

3.5 Design of the modules

The modules of the cable simulator need to be enclosed in a case that provides at least IP 20 protection from contact to live parts. Because the power supply Chroma 61602 [32] used to simulate effects of induced voltage is housed in $19''$, $3U$ rack mounted case, all the remaining modules should be also housed in $19''$ rack mounted cases to create a single system of the cable simulator.

To allow simple connection of all the modules together, all user accessible signal connectors should be 4 mm banana jacks. All the banana jacks used on the cable simulator should allow the connection of shrouded safety plugs to prevent contact of the user with potentially live wiring.

3.5.1 Transformer modules

To house the two power transformers a sufficiently large case needs to be used to fit the transformers and provide appropriate cooling. Because both transformers in a single case would exceed the 30 kg weight limit for any of the modules, each transformer will be placed in its own case. The case chosen, that is large enough to fit the transformer inside is a $19''$, $3U$ rack mounted case 1PS03PN from modushop.cz. The case itself weighs 4.4 kg. This weight combined with the weight of the transformers gives the total weight 27 kg including all the accessories.

The primary winding of the transformer should be equipped with voltmeter to monitor the set induced voltage and the secondary windings should be equipped with current meters to monitor the current flowing through the wires. The choice for the panel meters was such that both the voltmeter and the current meter should be able to operate without external power to minimize the wiring complexity.

The voltmeter for monitoring the induced voltage has been chosen to operate with voltages up to 300 V. The panel voltmeter PAN.V1060[3] has been chosen for the voltage monitoring. The accuracy class of the voltmeter is only 2.5 however because the voltmeter is expected to operate primarily as an indicator of proper operation, that no connected equipment is loading the transformer too much and that the circuit is wired correctly.

The current meter EQN72 1,5/3A[4] for monitoring the current flowing through the wires has been chosen with respect to the 1 A windings of the transformer. The current rating of the current meter is 1.5/3 A with fine scale to 1.5 A and indication of 3 A to monitor possible over current. The 1.5 A scale fits well with the transformer as the 1 A rating of the secondary winding is given by thermal effects of the current in the winding wire and short overloads don't pose a problem. The accuracy class 1.5 is sufficient for the current measurements.

To protect the transformer from longer over current scenarios a circuit breaker is placed in series with each secondary winding of the transformer. To minimize the area occupied on the front panel 2 A panel mounted circuit breakers in the shape of fuse holder[5] have been chosen. To protect the connected module from arcing caused by the inductance of the windings when the cables are disconnected while current flows

---

[3]Panelovy voltmetr AC, PAN.V1060 - http://www.tme.eu/cz/details/pan.v1060/panelova-meridla-analogova/

[4]Panelový ampérmetr AC, GOSSEN MULLER & WEIGERT EQN72 1,5/3A - http://www.tme.eu/cz/details/eqn72-1.5_3a/panelova-meridla-analogova/gossen-muller-weigert/eqn72-153a/

[5]Push to Reset Fuseholder-Type Thermal P&B Circuit Breaker - http://www.tme.eu/cz/Document/3a50e47f6fe702314a3316ea78ebecd0/W28.pdf

through the winding, all windings of the transformer are fitted with 350 *V* varistors to provide discharge path for the inductor current while having high impedance at lower voltages to prevent interference with the operation of the system.

The schematic of internal connections of the transformer module is in Fig. 25. Both modules are identical and are wired according to the same schematic.
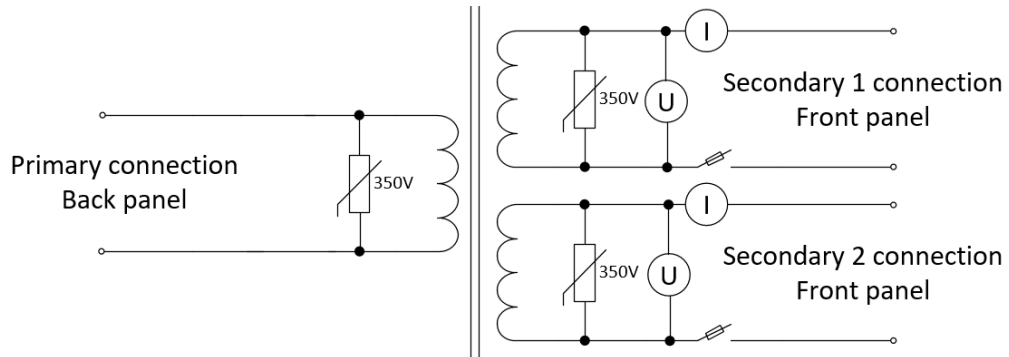
Figure 25 Schematic of the transformer module

The front panel of the transformer case needs to be modified to fit the connectors, panel meters to measure the voltage and current and circuit breakers to protect the transformer from over current. The expected layout of the front panel is shown in Fig. 26. The connection of the primary winding is not on the front panel because the power supply has its power outputs from the back so to minimize the wiring, it will be connected to the back of the transformer case.
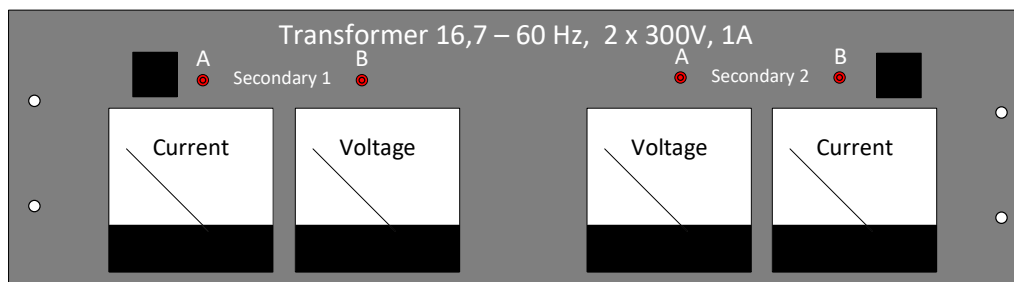
Figure 26 Layout of the front panel of the transformer module

3.5.2 Cable model module

To house the electronic circuits simulating the cables themselves the required case has been already chosen with respect to required thermal properties in Chapter 3.3 as a 3*U*, 19″ rack mounted case with heat sink sides 1PD03300N from modushop.cz to provide sufficient cooling to the resistors in the cable model.

The front panel of the cable model needs to be modified to allow the connection of the cables connecting the transformers in the cable and connecting the EUT and AE to the cable simulator. All the connections to the cable model module are realized from the front to be easilly accessible. The expected layout of the front panel of the cable simulator is in Fig. 27.
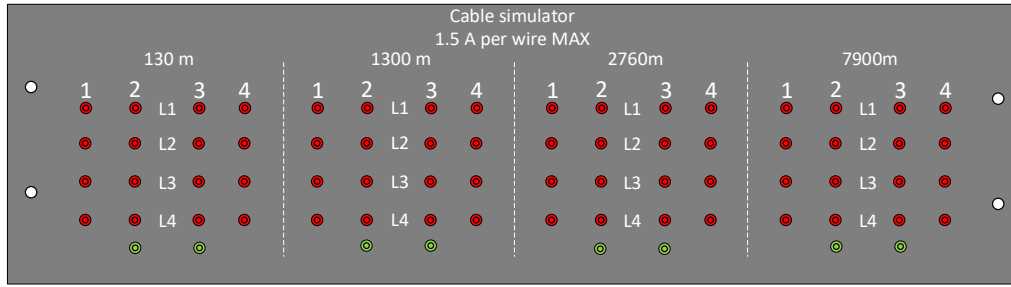
Figure 27 Layout of the front panel of the cable simulator case

The cable model module contains four printed circuit boards, one for each length of the simulated cable. The circuit boards are mounted to the bottom plate of the case by threaded spacers.

The principle schematic of single length wire of the cable model module is shown in Fig. 28. To support the connection of the induced voltage simulation transformer, the wiring is split in two blocks between which the transformer output may be connected. The wiring is the same for all the lengths of the wire, the only difference between the simulators of different length of the wire is that the shortest cable model has its resistors mounted on the printed circuit board and the longer cable models have the resistors mounted on the heat sinks of the case.
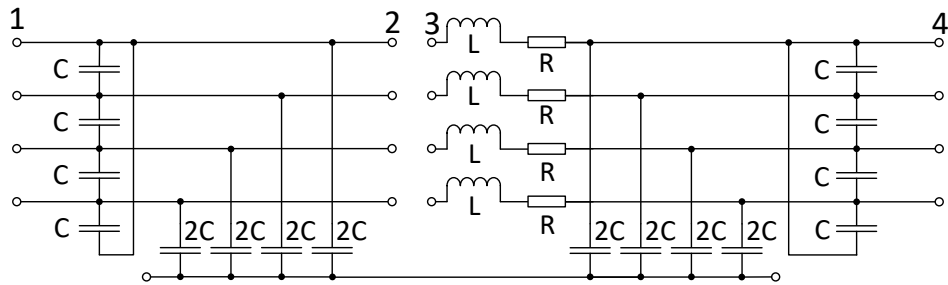
Figure 28 Principle schematic of the cable model for one length

3.6 Integration of modules

To assemble all the modules of the complete cable simulator and create a single unit a rack cabinet is chosen. This cabinet is required to hold all the components of the cable simulator and the power supply for providing the model of induced voltage.

All modules of the cable simulator are housed in metal cases. To assure the safety of operators, all the cases are connected to protective earth. This connection is assured by having an earhing point on each case, that is connected by a wire to the chassis of the rack cabinet. The rack cabinet shall be connected to protective earth by a power cord that is also used to power the cooling fans.

The stacking of modules in the rack cabinet is expected to be done in a way, that the heaviest transformers are mounted at the bottom. The power supply should be easily accessible to use it in other devices so it should be mounted at the top. This leaves the middle position for the cable model. The assembled rack will look according to Fig. 29.
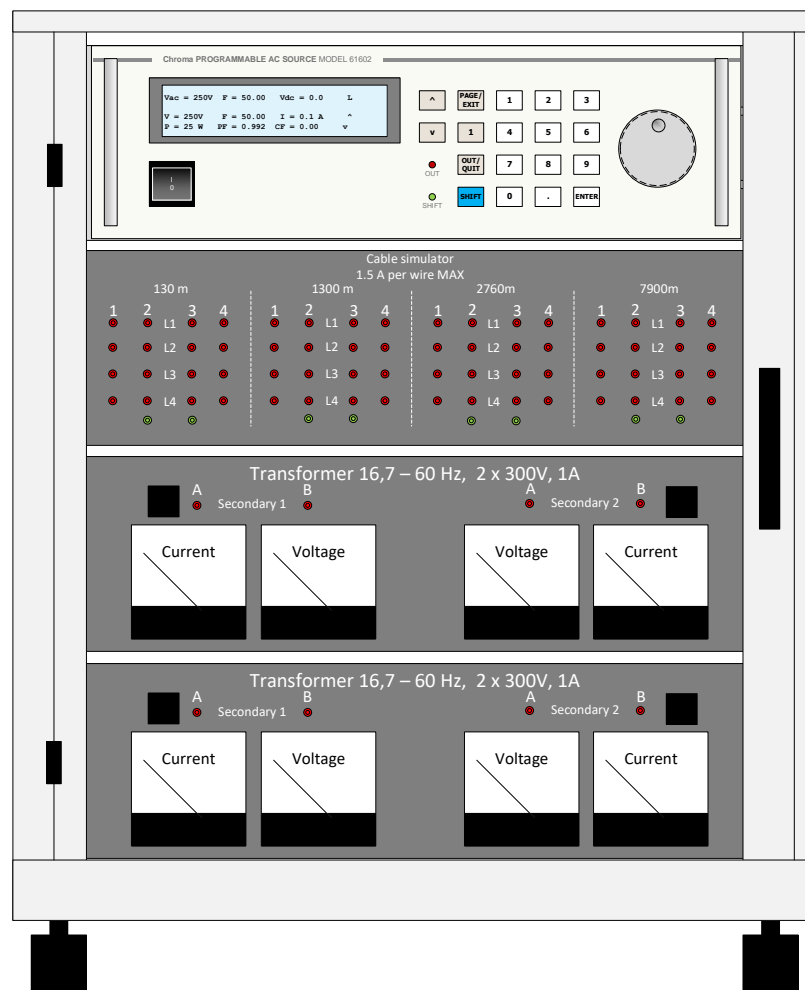

Figure 29 Stacking of the modules in the rack cabinet

The block diagram of all the modules of the cable simulator connected together with the tested device is shown in Fig. 30. All of the connections between the modules will be done from the front. The only exception is the connection between the power supply and the transformers. This connection is done in the back because the chosen power supply [32] has its output terminals on its back.
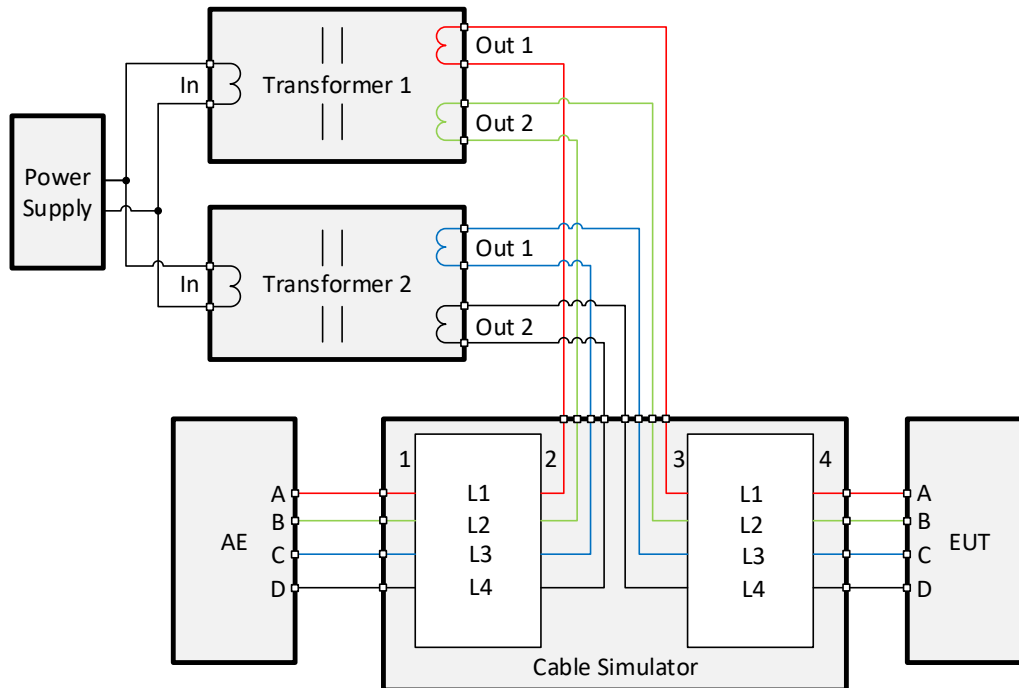
Figure 30 Stacking of the modules in the rack cabinet

The cable simulator can also be used for testing the devices without the effects of induced voltage. This is done by connecting the terminals 2 and 3 of the cable simulator together instead of to the transformers.

3.6.1 Choosing the rack cabinet

The rack cabinet must be able to hold both transformers, the cable model and the power supply. Each of the modules is housed in $3U$, $19''$ rack mounted case. The minimal height of the rack cabinet must therefore be $12U$. The transformers with the case weigh 27 kg each, the cable model in case weighs 10 kg and the power supply weighs 20 kg so the rack cabinet must be able to hold at least 84 kg.

To minimize the size of the rack cabinet, but provide enough space to insert shelves under the transformers a $15U$ closed rack cabinet Triton RMA 15 A66[6] with wheels for mobility of the cable simulator has been chosen. The load capacity of the rack is 400 kg so it should have no issue with the modules.

The rack cabinet is fully enclosed and prepared for grounding at a single point with all the metal parts electrically connected so the electrical safety of the operators of the cable simulator will not be an issue.

To provide the air flow needed for cooling of the modules a set of holes is expected to be drilled in the sides of the rack case. This approach has the advantage that the air used for cooling will be taken from outside the rack so it will not be affected by the heat transferred to it by the components of the cable simulator.

---

[6]TRITON Free-standing cabinet RMA - http://www.triton.cz/en/data-cabinets/free-standing-cabinets/free-standing-cabinet-rma

4 Verification of the circuit behavior

To model the behavior of the cable to have a baseline for comparison with the created cable simulator, a computer model in the LTSPICE [33] has been created. Because the components for the final model didn't arrive on time of delivering this work, a copy of the expected circuit of the hardware cable simulator with the components of the same values but lower voltage and current ratings, has been also created. This circuit is expected to behave very similarly to the final cable simulator to make a comparison between the hardware cable model with just single cable section and the computer model representing the real cable as close as possible.

4.1 Simple and complex models of the cable

To simulate the cable two electric models based on the parameters identified in chapter 2.1 have been created. One of the models is the same as for the cable simulator with single block of lumped parameters model. This model will be referred to as a simple model. Schematic of the simple cable model is already described in chapter 2.3. The second model is created as a distributed model consisting of 10 m sections of lumped model of the cable to provide more representative model of the real cable. This model will be referred to as a complex model. The desired length of the cable is built by connecting appropriate lengths of these cable sections. Schematic of a single 10 m cable section is shown in Fig. 31 and a generalized schematic of all the complex cables is shown in Fig. 32. The parameters of component values are set as shown in Tab. 13. The values are calculated from the total values found in chapter 2.1 and modified for the 10 m section length. The values of components for the simple model are the same as in the developed cable simulator. These values are shown in Tab. 8.
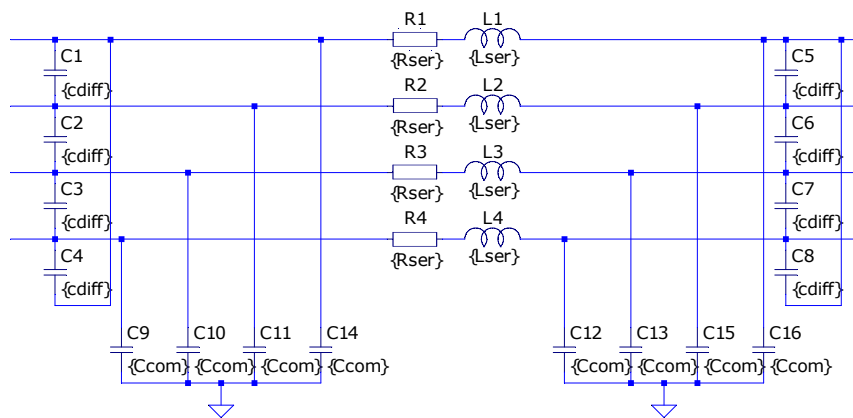

Figure 31 One 10 m element of the complex cable model

The complex model of the cable simulator has been done in the lengths of 130 m, 1300 m, 2 760 m and 7 900 m by connecting 13, 130, 276 and 790 of the 10 m cable segment in series.
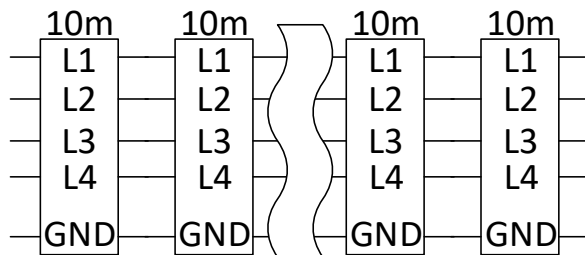
Figure 32 Generalized schematic of the complex cables

Table 13 Values of components in the complex cable computer simulation model (each 10 m section)

Parameter name	Value
C_{diff}	181.25 pF
C_{com}	362.5 pF
R_{ser}	72 $m\Omega$
L_{ser}	7.5 μH

4.2 Measurement and simulation of the cable simulator

The measurements were done on all the cable lengths: 130 m, 1 300 m, 2 760 m and 7 900 m. The tested hardware model of the cables of lengths 130 m, 1 300 m and 2 760 m is shown in Fig. 33. These cables behave close to the way the complete cable model would because they are based on components with the same values. The effect of the induced voltage is not measured in here because under normal operating conditions the induced voltage only stresses the insulation between lines and ground but has no effect on the behavior of the cable. This hardware model will be tested only at 20 V because the components used for the verification of circuit operation don't have the voltage rating to allow connection of higher voltages. The comparison was done against the simulations run on the computer models described in chapter 4.1. Measurements were done to identify a step response and a frequency response of the cable models.
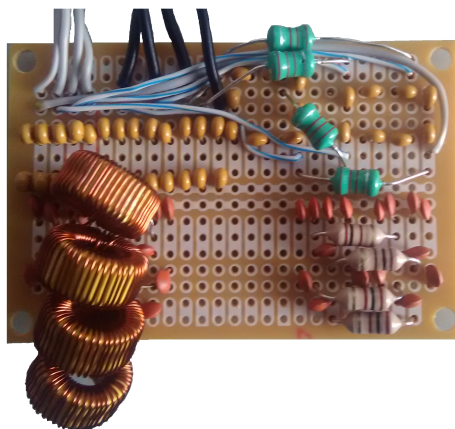

Figure 33 Measured circuit of a 130 m, 1 300 m and 2 760 m cables

4.2.1 Step response of the cable

The step response of the cable was measured by connecting the cable model to a signal generator with power output. Both input and output of the cable were measured to obtain the response and correctly determine the rise and fall times to run the simulation under the same conditions. The connection diagram for measurement of the response is shown in Fig. 34. The unused two wires of the cable simulator are shorted together on both ends to provide the same effect as a low impedance supply and load would have. The responses are measured for low impedance input and high impedance output to simulate connection to input of communication equipment.
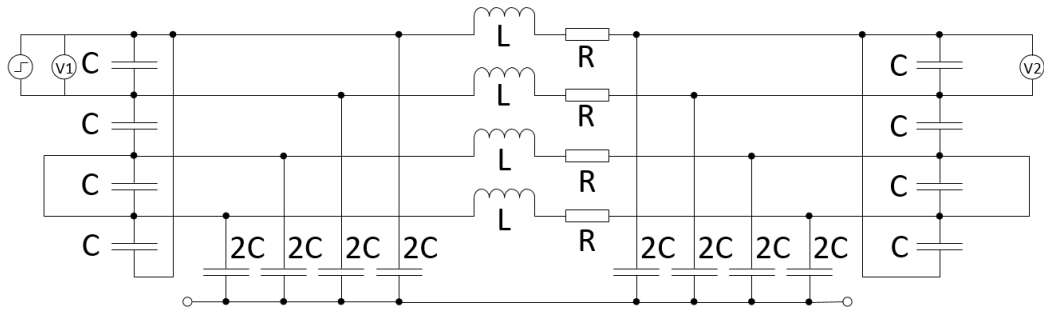
Figure 34 Connection diagram for the cable response measurement

The simulated step response of the unloaded cables for lengths from 130 m to 7 900 m is shown in Figures 35 to 43.
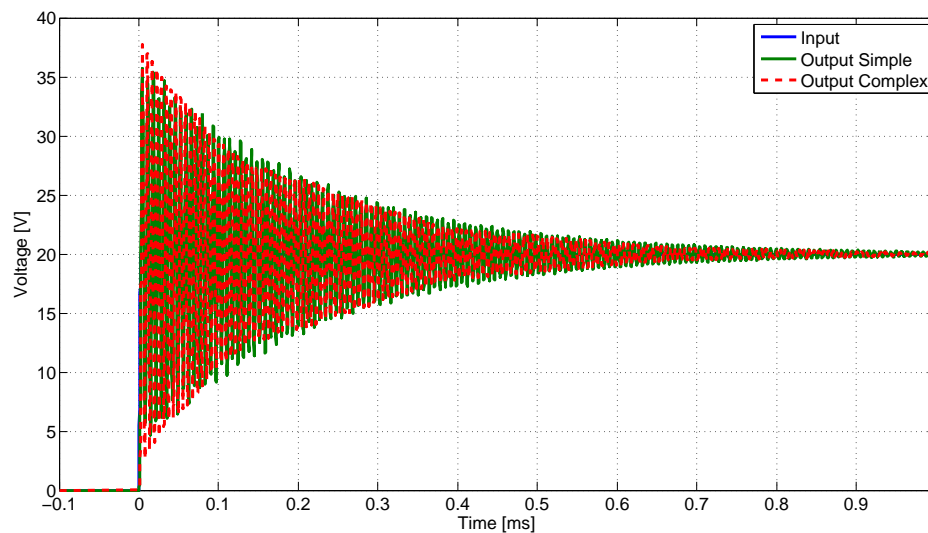

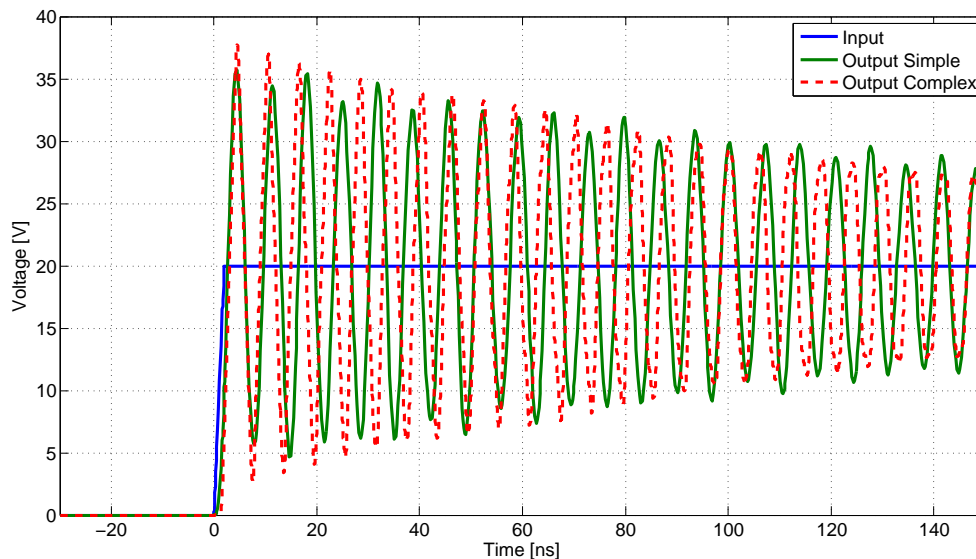**Figure 35** Simulated step response of the 130 m cable

Figure 36 Detail of the simulated step response of the 130 m cable
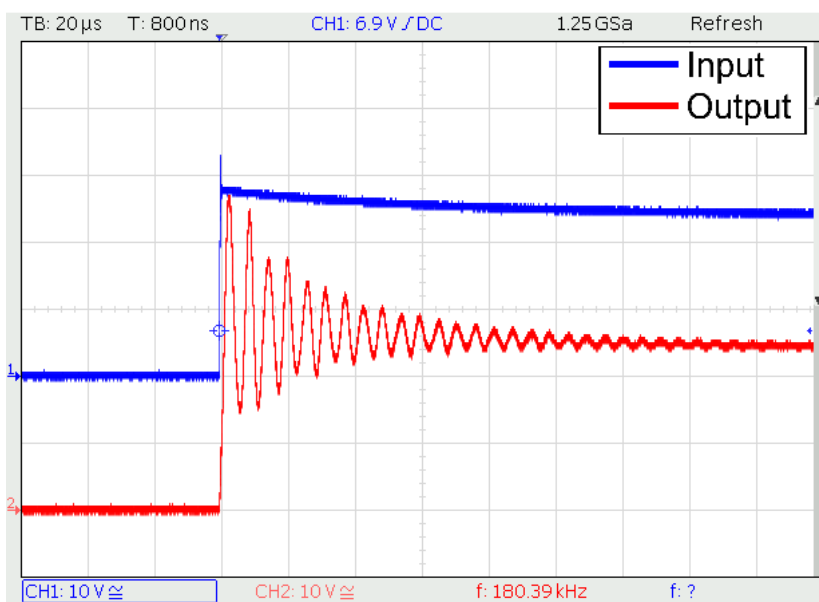

Figure 37 Measured step response of the 130 m cable circuit

The simulations show that both the simple and the complex computer simulations of the 130 m cable behave almost identically as shown in Fig. 35. The measured oscillations after the step decay three times as as fast as in the simulated version but the frequency of the oscillations matches the simulation. This is mostly caused by the equivalent series resistance (ESR) of the capacitors dampening the circuit more than was expected. The effect of the ESR of the capacitors will be discussed later. The detail of simulated step response is shown in Fig. 36. This shows that the complex

model oscillates at higher frequency than the simple model. The measured frequency of oscillations is the same as the frequency of oscillations of the complex model.
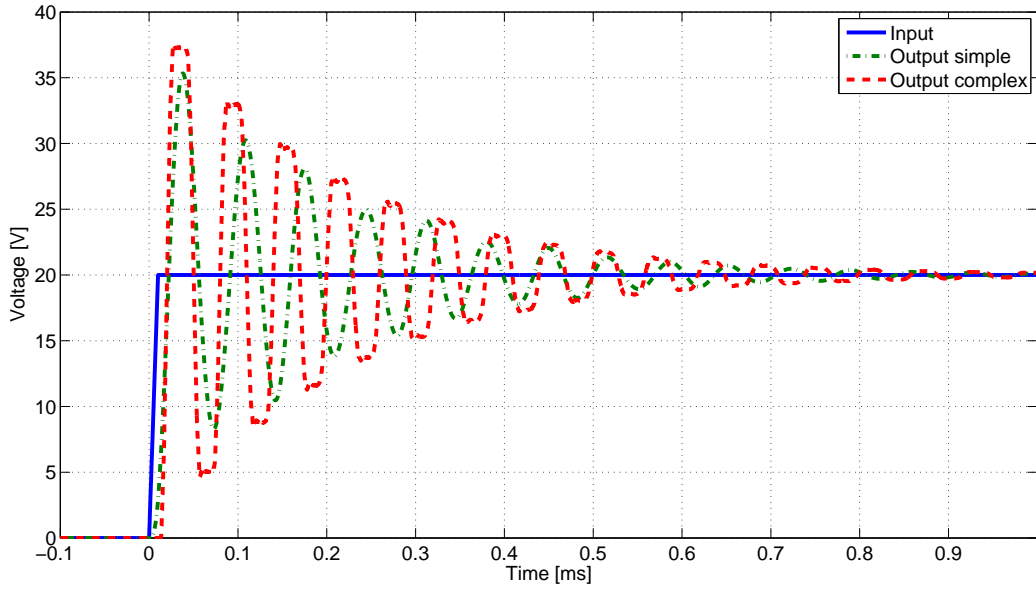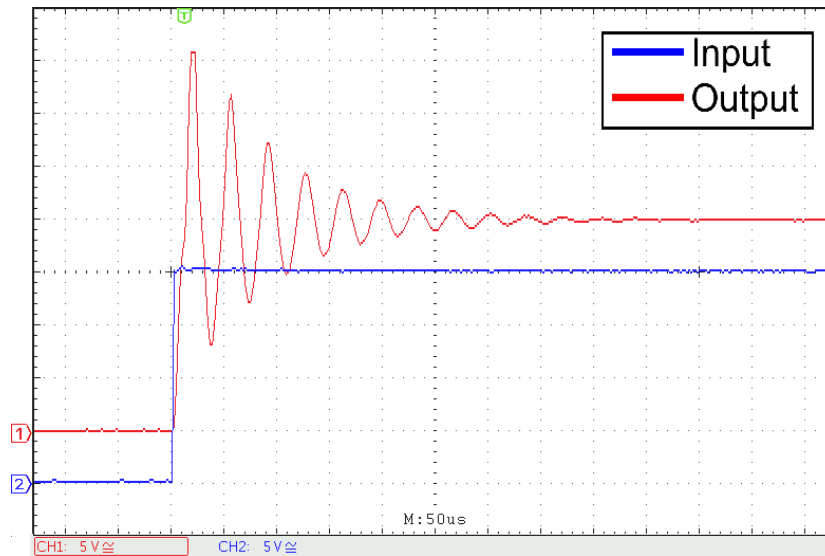

Figure 38 Simulated step response of the 1 300 m cable

Figure 39 Measured step response of the 1 300 m cable circuit

The 1 350 m simulations show a difference in behavior between the simple and the complex model. The simple model only exhibits dampened oscillations while the complex model shows reflections from the ends of the cable. The dampened oscillations of the simpler model are slower than the the reflections in the more complex model but the amplitude and rate of decay of the oscillations is very similar. Measurement shows the same amplitude of overshoot but the rate of decay of the oscillations is again faster than the simulated. The difference in the rate of decay is smaller than in the case of the 130 m cable, only decaying abut 1.5 times as fast as the simulations because the capacitors have higher capacitance to ESR ratio.
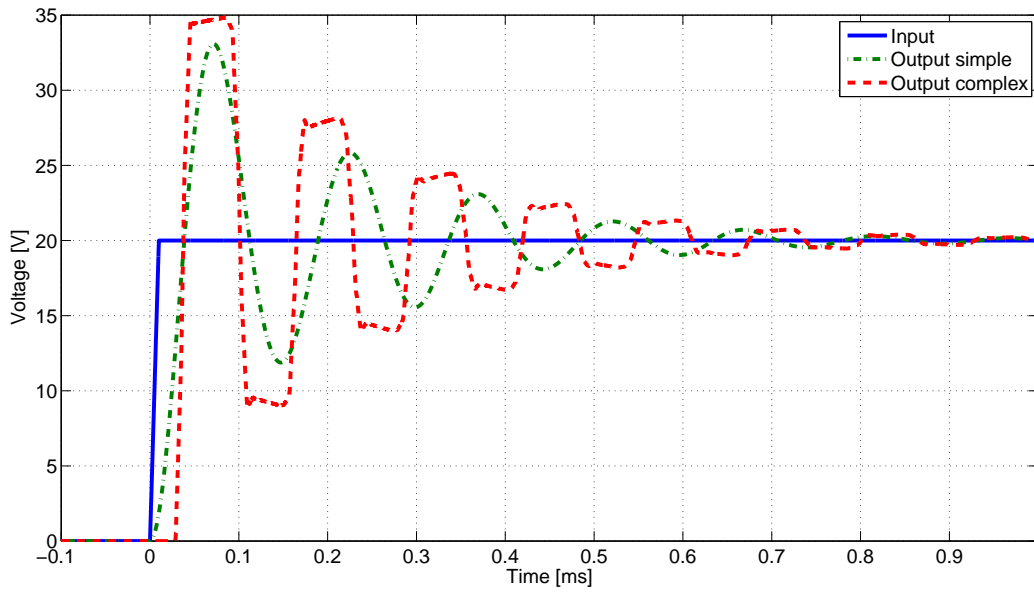
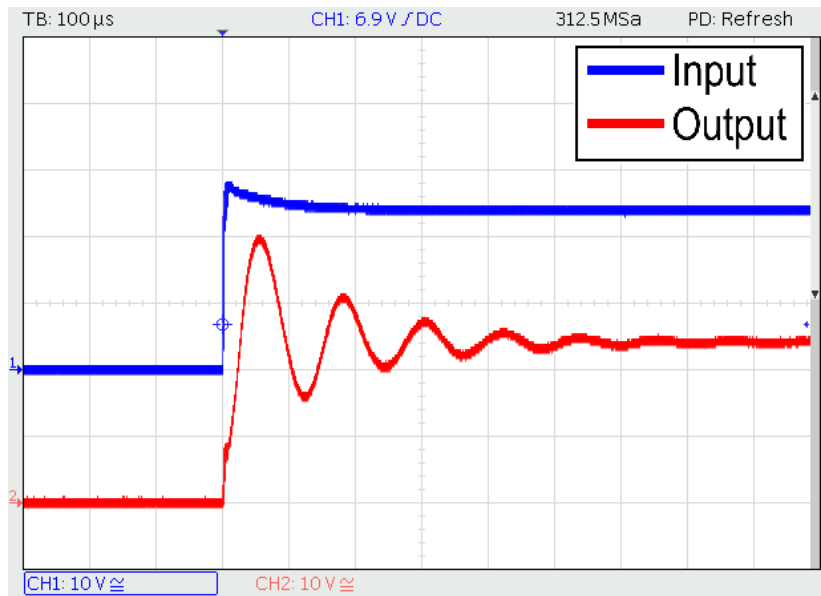**Figure 40** Simulated step response of the 2 760 m cable

Figure 41 Measured step response of the 2 760 m cable circuit

The results of the simulations of the 2 760 m cable exhibit the same difference between the simple and complex model as in the 1 300 m case. The overshoot and the oscillation decay rates of the measured model are close to the simulation of the simple model.
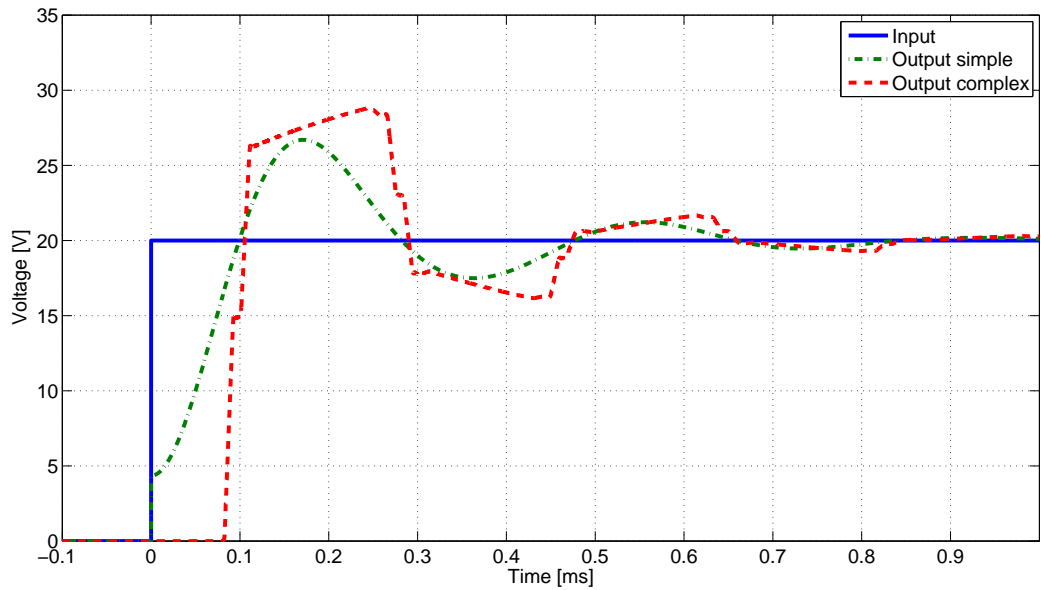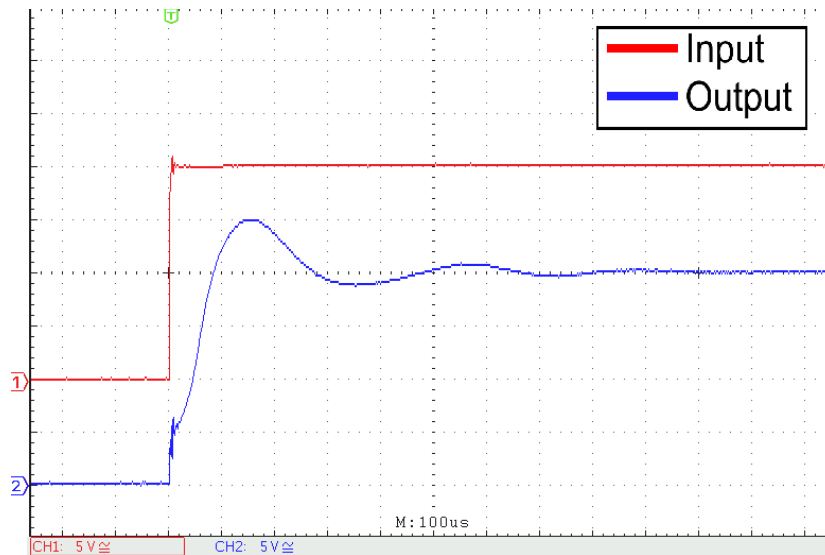
Figure 42 Simulated step response of the 7 900 *m* cable

Figure 43 Measured step response of the 7 900 *m* cable circuit

Behavior of the simulated 7 900 *m* cables shows that at this length the reflections in the cable are getting dampened much more than in the shorter cables. The frequency of the oscillations and the reflections match well. The measured response corresponds to the simulation of the simple model with having slightly smaller amplitude of the oscillations but the same frequency and decay of the oscillations.

To verify the effect of the equivalent series resistance of the capacitors, the computer simulation of the simple model of the 130 *m* cable has been run with the same ESR as was measured on the capacitors. The results of the simulation are shown in Fig. 44. The simulation results show the same faster decay of the oscillations as was observed in the measurements.
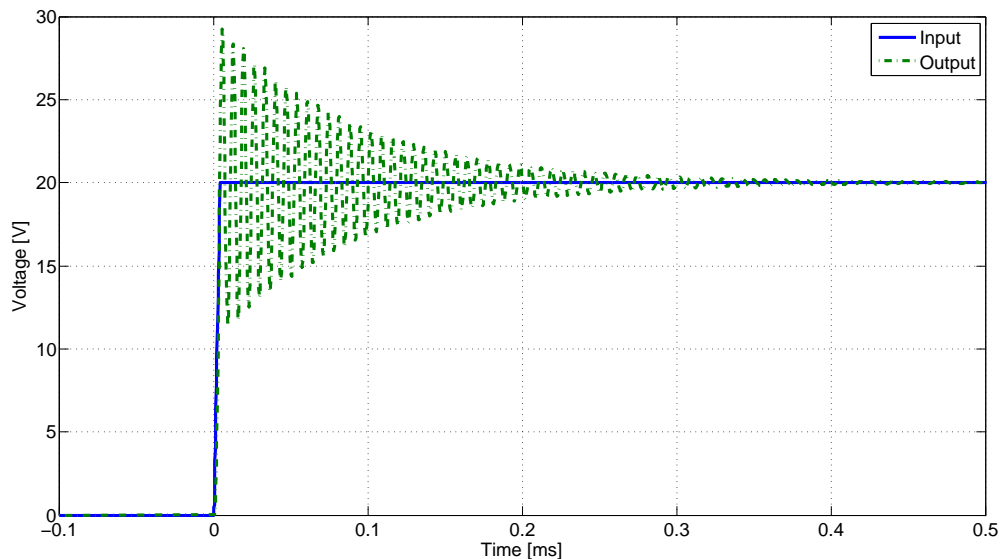
Figure 44 Simulated step response of the 130 *m* cable with added ESR of the capacitors

The step response measurement shows that the cable simulator hardware performs close to what can be expected from a real cable of the same length. The amplitude of the initial overshoot fits within a few percent to the simulated value so the connected equipment will experience similar operating conditions as when it would be connected to a real cable. The decay of the oscillations is faster than what is simulated for ideal capacitors with no ESR however the final cable simulator will be built with capacitors that have lower ESR so the difference will be smaller.

4.2.2 Frequency response of the cable

To characterize the behavior of the created hardware cable simulator across the frequency range a response of the cable has been measured. The connection diagram is the same as in measuring the step response as shown in Fig. 34 where the step generator is substituted by function generator and sweeping the input frequency. Because the step response of the simple simulation model and measured hardware cable model are close to each other, only the complex computer model was simulated to get a comparison between the created cable simulator and the real cable. The beginning of the sweep was chosen at 10 *Hz* to cover the low frequency behavior. The upper frequency was chosen to be approximately one decade above the resonant frequency of the cable.

The results of the simulations and measurements are shown in Fig. 45 to Fig. 48. The shortest 130 *m* cable has the highest resonance frequency about 2 *MHz* and the longest 7 900 *m* cable has the lowest resonant frequency only about 3 *kHz* . The simulations of the two shorter cables show that the resonant frequency of the cable model is about 10 % higher than the resonant frequency of the cable obtained from simulation. The measurements for the 2760 *m* cable show that the resonant frequency is exactly the same as shown in Fig. 47. The measurements also show that the voltage transfer ratio for frequencies above the resonant frequency is much lower on the created cable models
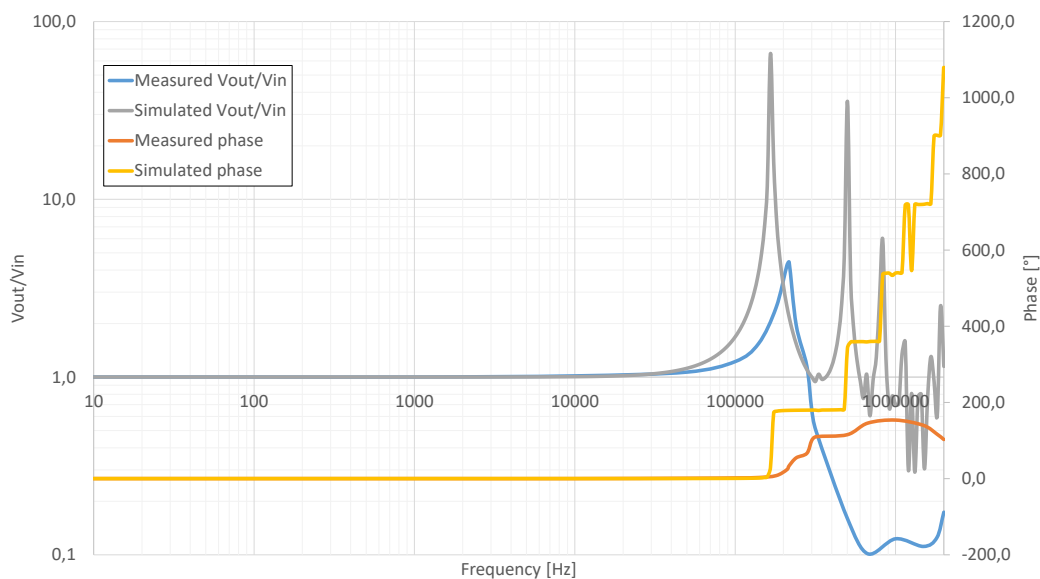
than on the simulated cable.

Figure 45 Simulated and measured frequency response of the 130 m cable
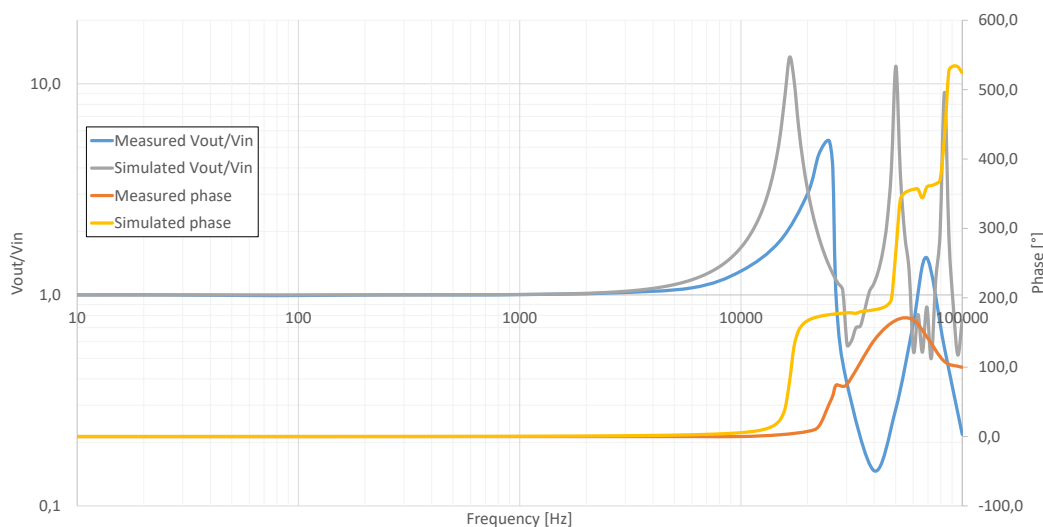

Figure 46 Simulated and measured frequency response of the 1 300 m cable

The phase behavior is different between the measurements and simulations for signals with frequency higher than the resonant frequency of the cable. The difference is caused by the fact that the simulated cable was created by many lumped elements of short cable connected in series and the measurements were done on a single lumped element of the entire length of the cable. To keep the behavior of the cables as close to the expected behavior, only signals with frequency content up to 1 kHz should be used.
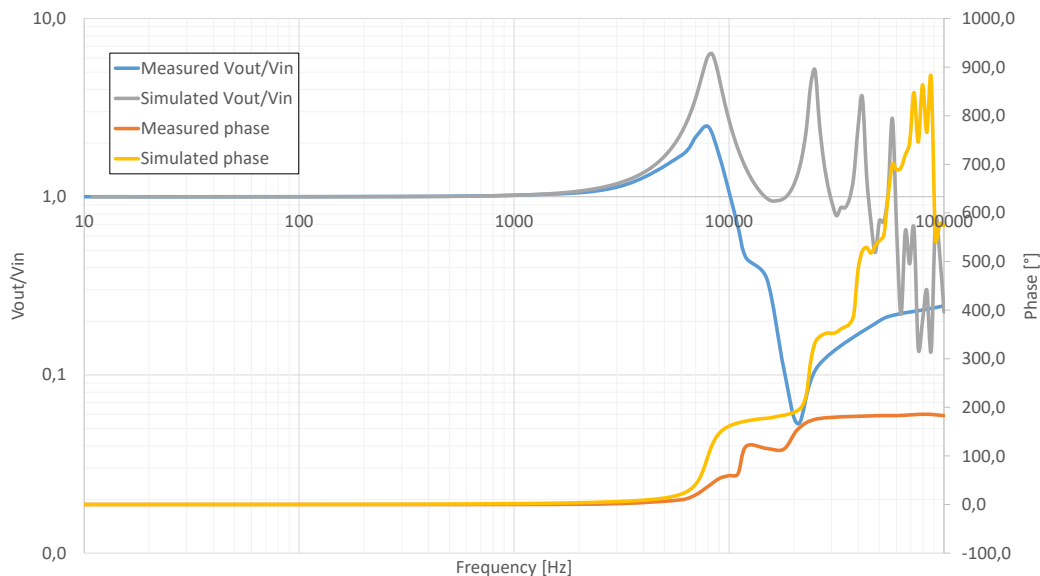
Figure 47 Simulated and measured frequency response of the 2 760 m cable
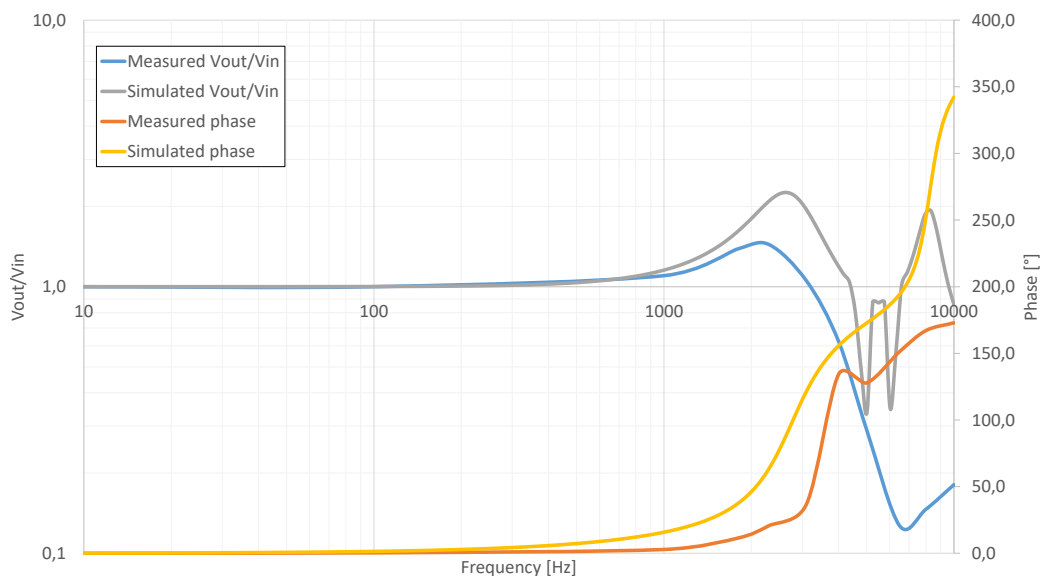
Figure 48 Simulated and measured frequency response of the 7 900 m cable

The amplitude behavior of the measured cable shows that the the transmitted signal at resonance frequency is more dampened than what was simulated for an ideal model. This dampening is caused by the ESR of the capacitors and core losses in used inductors. The behavior at frequencies higher than the resonance frequency differs because the entire cable has been substituted with only a single element of the lumped model.

4.3 Evaluation of the measured data

Measurements of the step response of the cables show that the amplitude of overshoot after a step input is presented is the same as in computer simulations of the cable. The rate of decay of the oscillations is faster than expected by the computer simulations. This difference is caused by ESR of the capacitors and verified by running a simulation where the ESR of the capacitors has been included.

The measurements show that the resonant frequency of the created cable simulator corresponds well to the results of computer simulations. The simulated and measured resonant frequencies for each length of the cable are summarized in Tab. 14. The phase and amplitude behavior for frequencies below the resonant frequency differs negligibly however at frequencies higher than the resonant frequency of the cable both the phase and amplitude behavior don't match the simulation because the simple created model cannot accurately describe the reflections at the ends of the cable. Therefore the cables should only be used with signals that don't contain frequencies above $1 \, kHz$.

Table 14 Overview of the resonant frequencies of the cable

Cable length $[m]$	130	1 300	2 760	7 900
Simulated resonant frequency $[kHz]$	180	18	8.2	2.7
Measured resonant frequency $[kHz]$	210	26	8.0	2.2

5 Conclusion

Within this thesis, the theoretical analysis of the issues of simulating cables placed along an electrified railway track, have been examined. The characteristics of the cables regarding the inductance, capacitance and resistance has been described in chapter 2.1. Based on these parameters the model of the cable has been created and the cable simulator has been designed to represent the cable model as closely as possible within the confined area of the cable simulator so that the cable simulator can be used instead of the field tests of developed equipment.

The effect of induced disturbing voltages for cables placed along an electrified track has been examined. Based on the findings and description of normative references a maximum value of the induced voltage has been estimated at 300 V_{RMS}. To inject the induced voltage in the cable a transformer capable of operating at 16.7 Hz and 300 V has been designed. This transformer can be connected in the midpoint of the cable simulator to add the effect of the induced voltage.

The cable simulator has been designed to fit in a set of rack mounted cases. The stacking of the cases has been considered and the complete cable simulator has been designed to fit in a standard 15 U rack cabinet to create a single functional module.

The designed cable simulator has not been completed in its full scale due to issues in order placement and processing. To verify the operation and make measurements on the cable simulator a smaller version of the cable model has been created to compare the responses of the simulated cable consisting of many 10 m blocks with the designed cable simulator.

By measuring the frequency response and the step response of the different lengths of the cable simulator and comparing the results with the simulation, it was verified, that the step response of the cable simulator closely resembles the expected step response. The frequency response shows very similarly located first resonance frequency however the behavior of the measurements and the simulations start to differ at higher frequencies. The expected operation of the cable simulator is with signals at lower frequencies and so the resemblance of the responses is sufficient.

References

[1] *Drážní zařízení - Elektromagnetická kompatibilita - Část 4: Emise a odolnost zabezpečovacích a sdělovacích zařízení.* Standard ČSN EN 50121-4. Prague, CZ: Český normalizační institut, Jan. 2016.

[2] *Elektrische Bahn-Signalanlagen.* Standard DIN VDE 0831. Aug. 1990.

[3] *Beeinflussung und Schutzmaßnahmen - Grenzwerte der Beeinflussung.* Standard RIL 819.0804. Dec. 1996.

[4] Nexans. *Railways signalling cables.* URL: http://www.nexans.co.uk/UK/group/doc/en/Railways%20Signalling%20-%20Iberia.pdf (visited on 01/18/2017).

[5] Caledonian. *Railways signalling cables.* URL: http://www.caledonian-cables.co.uk/docs/railway/Railway%20Cables.pdf (visited on 01/18/2017).

[6] Institution of railway signal engineers. *Signalling and telecommunications cables for use on minor railways.* URL: http://www.irse.org/minorrailways/publicdocuments/CA01%20Cables%20v1.0.pdf (visited on 01/18/2017).

[7] Muhammad H Rashid. *Power electronics handbook.* Elsevier Science, 2011.

[8] Marc T Thompson. "Inductance Calculation Techniques—Approximations and Handbook Methods". In: *Power Control Intelligent Motion* (1991).

[9] Sushil Kumar Ganguli and Vivek Kohli. *Power Cable Technology.* CRC Press, 2016.

[10] D. C. Meeker. *Finite Element Method Magnetics, Version 4.2.* URL: http://www.femm.info.

[11] University of California at Berkeley. *Triangle: A Two-Dimensional Quality Mesh Generator and Delaunay Triangulator.* URL: https://www.cs.cmu.edu/~quake/triangle.html (visited on 05/08/2017).

[12] Kabedex. *Kolejnice a výhybky.* URL: http://www.kabedex.cz/files/files_34201192.pdf (visited on 04/30/2017).

[13] Roberto Cella et al. "Measurement of AT electric railway system currents at power-supply frequency and validation of a multiconductor transmission-line model". In: *IEEE Transactions on Power Delivery* 21.3 (2006), pp. 1721–1726.

[14] *Drážní zařízení - Napájení a drážní vozidla - Technická kritéria pro koordinaci mezi napájením (napájecí stanicí) a drážními vozidly pro dosažení interoperability.* Standard ČSN EN 50388. Prague, CZ: Český normalizační institut, Mar. 2006.

[15] Jim Lux. *Soil Dielectric Properties.* URL: http://pe2bz.philpem.me.uk/Comm/-%20Antenna/Info-905-Misc/soildiel.htm (visited on 01/18/2017).

[16] Ward E Patitz, Billy C Brock, and Edward G Powell. "Measurement of Dielectric and Magnetic Properties of Soil". In: ().

[17] B Mellit et al. "Computer-based methods for induced-voltage calculations in AC railways". In: *IEE Proceedings B-Electric Power Applications.* Vol. 137. 1. IET. 1990, pp. 59–72.

References

[18] BattIndustrial. *Network Rail Signal Cable*. URL: `http://www.batt.co.uk/upload/files/c3%5C_1231338097.pdf` (visited on 04/30/2017).

[19] Lazar Rozenblat. *CALCULATING SPACING BETWEEN PCB TRACES FOR VARIOUS VOLTAGE LEVELS*. URL: `http://www.smps.us/pcbtracespacing.html` (visited on 05/13/2017).

[20] *Information Technology Equipment – Safety – Part 1: General Requirements*. Standard UL 60950-1. Northbrook, IL: Underwriters Laboratories Inc. (UL), Mar. 2007.

[21] Lazar Rozenblat. *PCB CREEPAGE CALCULATOR*. URL: `http://pcbdesign.smps.us/creepage.html` (visited on 05/13/2017).

[22] *Generic Standard on Printed Board Design*. Standard IPC-2221B. Bannockburn, IL: IPC, Nov. 2012.

[23] LLC Engineers Edge. *Convective Heat Transfer Coefficients Table Chart*. URL: `http://www.brighthubengineering.com/hvac/92660-natural-convection-heat-transfer-coefficient-estimation-calculations/` (visited on 05/07/2017).

[24] Bright Hub Engineering. *Natural Convection Heat Transfer Coefficient*. URL: `http://www.engineeringtoolbox.com/convective-heat-transfer-d_430.html` (visited on 04/30/2017).

[25] The Engineering ToolBox. *Air Properties*. URL: `http://www.engineeringtoolbox.com/air-properties-d_156.html` (visited on 04/30/2017).

[26] Engineer Experiences. *Calculations for Design Parameters of Transformer*. URL: `http://engineerexperiences.com/design-calculations.html` (visited on 05/06/2017).

[27] Engineer Experiences. *Turns per Volts Derivation Transformer Design*. URL: `http://engineerexperiences.com/turns-per-volts-transformer-design.html` (visited on 05/06/2017).

[28] Semic Trade. *Silicon steel cores*. URL: `http://www.semic.cz/!KATEGORIE/6K/Catalogue%20Silicon%20steel%20cores.pdf` (visited on 05/05/2017).

[29] R. Nave. *Approximate Inductance of a Toroid*. URL: `http://hyperphysics.phy-astr.gsu.edu/hbase/magnetic/indtor.html` (visited on 05/07/2017).

[30] McLyman $\kappa\alpha\iota$ Colonel. "Window Utilization, Magnet Wire and Insulation". In: $\sigma\varepsilon$ *Transformer and Inductor Design Handbook, Idyllwild, Ca, USA, Marcel Dekker Inc* (2004).

[31] 3M. *3M Electrical Tapes*. URL: `https://multimedia.3m.com/mws/media/103938O/3m-oem-insulating-and-conductive-tapes-brochure.pdf` (visited on 05/08/2017).

[32] Chroma. *Programmable AC Power Source*. URL: `http://www.chromausa.com/pdf/Br-61600-acsource-112012.pdf` (visited on 05/12/2017).

[33] IV LTspice and Device Models. *Linear Technology*. 2013.